

APP: Accelerated Path Patching with Task-Specific Pruning

Frauke Andersen^{*1}, William Rudman^{*2}, Ruochen Zhang^{*3},
Carsten Eickhoff¹

¹University of Tübingen, ²The University of Texas at Austin, ³Brown University
william.rudman@utexas.edu

Abstract

Circuit discovery is a key step in many mechanistic interpretability pipelines. Current methods, such as Path Patching, are computationally expensive and have limited in-depth circuit analysis for smaller models. In this study, we propose *Accelerated Path Patching* (APP), a hybrid approach leveraging our novel *contrastive* attention head pruning method to drastically reduce the search space of circuit discovery methods. Our Contrastive-FLAP pruning algorithm uses techniques from causal mediation analysis to assign higher pruning scores to task-specific attention heads, leading to higher performing sparse models compared to traditional pruning techniques. Although Contrastive-FLAP is successful at preserving task-specific heads that existing pruning algorithms remove at low sparsity ratios, the circuits found by Contrastive-FLAP alone are too large to satisfy the minimality constraint required in circuit analysis. APP first applies Contrastive-FLAP to reduce the search space on required for circuit discovery algorithms by, on average, 56%. Next, APP, applies traditional Path Patching on the remaining attention heads, leading to a speed up of 59.63%-93.27% compared to Path Patching applied to the dense model. Despite the substantial computational saving that APP provides, circuits obtained from APP exhibit substantial overlap and similar performance to previously established Path Patching circuits.^{1 2}

1 Introduction

A central focus of mechanistic interpretability research (Elhage et al., 2021; Olah, 2022) is the study of minimal subgraphs, or circuits, within Large Language Models (LLMs) to identify the internal mechanisms responsible for particular functions (Elhage et al., 2021; Olah, 2022). Circuits consist of subsets of model components, such as

attention heads or feed-forward layers, that can largely account for a model’s performance on certain tasks (Vig et al., 2020; Wang et al., 2022; Hanna et al., 2023). Locating these components within a highly overparameterized LLM is computationally expensive. To verify whether a particular component belongs to a circuit, recent studies employ techniques such as Path Patching (Goldowsky-Dill et al., 2023a; Wang et al., 2022), which requires multiple model runs to measure the causal effects of individual components. Since this process must be repeated for *every component* to fully outline a circuit, it quickly becomes prohibitively costly as we increase the number of parameters in a model.

The objective of identifying a minimal, well-performing subnetwork aligns with pruning (Frankle and Carbin, 2018), which seeks to improve model efficiency by removing uninformative model components. Unlike circuit discovery methods, many pruning algorithms are computationally efficient, requiring only a few forward passes and using weight- or activation-based heuristics (Zhu et al., 2024; Sun et al., 2024) to remove unimportant model components. In this paper, we explore the connection between Path Patching and unstructured pruning (Frantar and Alistarh, 2023; Sun et al., 2024; An et al., 2024) that are adapted to preserve full-attention heads, rather than focusing on algorithms that target individual model weights (Zhu et al., 2024). Specifically, we employ FLAP (An et al., 2024) to investigate whether pruning alone can recover minimal circuits. We demonstrate that, under the same performance budget, circuits obtained through pruning are significantly larger than those identified via path patching. Namely, pruning cannot truly recover *minimal* circuits.

By comparing FLAP-generated circuits to those produced by Path Patching, we observe that FLAP often removes task-specific heads that are critical

¹Equal contribution. Order determined by coin flip.

²Code: <https://github.com/FraukeAcceleratedPathPatching>

for subnetwork performance. These task-specific heads only activate when exposed to a particular input and often implement specialized, interpretable functions. Although pruning alone cannot reduce an LLM to its minimal subnetwork, it can serve as an effective preprocessing step that substantially *reduces* the search space for circuit discovery. Building on this insight, we propose Accelerated Path Patching (APP), which incorporates pruning our novel Contrastive-FLAP pruning algorithm as a preliminary stage of the patching process. Contrastive-FLAP utilizes the contrastive minimal-pair setup commonly used in causal mediation analysis to target task-specific heads found by Path Patching. Using APP for circuit discovery recovers minimal circuits with comparable performance to Path Patching while reduces computational costs by up to 93%.

Our main contributions are as follows:

- We provide a detailed analysis of the differences between path patching and the most closely related attention-head pruning algorithm, FLAP, showing that pruning alone fails to recover minimal circuits.
- We propose Contrastive-FLAP to better preserve task-specific attention heads that are otherwise pruned at low sparsity ratios.
- We replace the original Path Patching search space with the union set identified by Contrastive-FLAP and FLAP. By incorporating pruning as a prior step, we introduce APP, which significantly reduces search cost while faithfully recovering minimal circuits.

2 Related Work

2.1 Circuits

In transformer models, circuits refer to computational subgraphs that implement specific, often human-interpretable, behaviors (Olah et al., 2020). Depending on the level of granularity, nodes in these graphs may correspond to attention heads, MLPs, or even individual query, key, and value activations (Conmy et al., 2023). Edges typically represent residual connections, linear projections on the residual stream, or interactions within attention and MLP blocks (Elhage et al., 2021).

Path patching is one of the most widely used techniques for circuit discovery (Vig et al., 2020; Geiger et al., 2021; Wang et al., 2022; Hanna et al.,

2023). The method localizes model components that causally influence the output by contrasting clean and corrupted input pairs. It involves caching activations for both inputs and selectively replacing the activations of individual components (e.g., heads) in the clean run with those from the corrupted run. This process identifies components whose intervention most significantly alters the final logits. When combined with logit attribution techniques (Nostalgebraist, 2020; Yu et al., 2023; Zhang et al., 2024; Golovanevsky et al., 2025), path patching enables fine-grained functional interpretations of model behavior. For instance, in the IOI (Indirect Object Identification) task, Wang et al. (2022) identify interpretable head types such as previous token heads and name mover heads.

However, circuit discovery still remains computationally expensive. Recent methods like ACDC (Conmy et al., 2023) aim to automate this process by iteratively applying activation patching while pruning components with sub-threshold effects. However, circuits discovered via such automated approaches can be noisy and may omit components whose contributions to the logits negatively impact model performance. Other works (Syed et al., 2023; Hanna et al., 2024) explore related automated techniques focusing on edge-level localization rather than component-level discovery, which is a complementary but distinct research focus from this paper.

2.2 Pruning

Pruning refers to the process of reducing a model’s size or computational complexity while preserving overall performance. It can be broadly categorized as unstructured, semi-structured, or structured (Zhu et al., 2024). Unstructured pruning (Sun et al., 2024; Frantar and Alistarh, 2023) removes individual parameters, resulting in irregular sparse connectivity that often requires retraining or specialized sparse kernels when applied at high sparsity. Structured pruning, in contrast, removes entire model components, such as attention heads (An et al., 2024), channels (Ma et al., 2023), or even full layers (Fan et al., 2019), yielding more hardware-efficient architectures. Semi-structured pruning combines aspects of both approaches.

Since our goal is to compare pruning methods that operate at the attention-head level, similar to circuit discovery via path patching, we focus on structured, one-shot pruning techniques, specifically Fluctuation-based Adaptive Structured Prun-

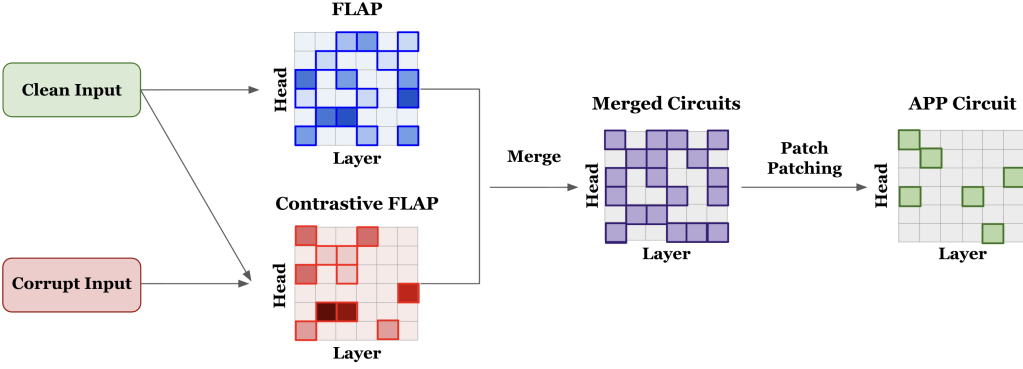


Figure 1: Depiction of the Accelerated Path Patching (APP) Algorithm. APP reduces the search space of circuit discovery methods by successfully pruning task-irrelevant heads while preserving task-critical attention heads. APP then runs Path Patching on the remaining sparse model.

Task	Prompt	Corrupted Prompt	$LD = L(\text{correct}) - L(\text{wrong})$
IOI	When John and Mary went to the store, John bought a drink for ...	When John and Mary went to the store, Alex bought a drink for ...	$L(\text{Mary}) - L(\text{John})$
Greater Than	The war lasted from 1873 to 18...	The war lasted from 1801 to 18...	$L(\{x (x > 73) \wedge (x \leq 98)\}) - L(\{x x \leq 73\})$
Gendered Pronouns	So Emily is such a good friend, isn't ...	That Person is such a good friend, isn't ...	$L(\text{she}) - L(\text{he})$
Induction	Today, Claire visited the library. There Cl...	Today, Claire visited the library. There Tr...	$L(\text{aire}) - L(\text{istan})$
Docstring	def old(self, first, page, names, size, files, read): """sector gap population :param page: message tree :param names: detail mine :param ...	def old(self, first, project, target, new, files, read): """sector gap population :param image: message tree :param update: detail mine :param	Wrong Variables = $\{ \text{first}, \text{page}, \text{names}, \text{files}, \text{read}, \text{project}, \text{target}, \text{new} \}$ $L(\text{size}) - \arg \max_{x \in \text{Wrong Variables}} L(x)$

Table 1: Example prompts and the logit differences for all five tasks used in this work. Logit Difference (LD) is defined by the difference between the logits of the correct and wrong answer.

ing (FLAP) (An et al., 2024). FLAP eliminates the need for retraining by computing an importance score for each attention head, which integrates both weight magnitude and activation statistics (Sun et al., 2024). Heads with the lowest scores are pruned iteratively until a target sparsity ratio is reached. Finally, FLAP introduces a bias correction term to each layer to mitigate pruning-induced errors. In this work, we omit this final correction step, as our objective is to use the pruning decisions themselves to identify functionally important components for circuit discovery.

3 Methodology

3.1 Experimental Setup

Models & Tasks In this paper, we conduct all patching experiments using four models: GPT-2 Small, GPT-2 Large, Qwen2.5-0.5B, and Qwen2.5-7B. We include the GPT-2 family (Radford et al., 2019) since it has been extensively used in prior mechanistic interpretability research, and well-characterized circuits have been identified in GPT-2 Small. The Qwen2.5 models (Yang et al., 2024) are selected for their strong performance across a range of downstream tasks. We evaluate these models on

five benchmark tasks commonly used in mechanistic interpretability: Indirect Object Identification (IOI) (Wang et al., 2022), Greater Than (Hanna et al., 2023), Gendered Pronouns (Mathwin et al., 2023), Induction (Goldowsky-Dill et al., 2023b), and Docstring (Heimersheim and Janiak). Each of these tasks contains a paired clean set $\mathcal{D}^{\text{clean}}$ and a corrupted set $\mathcal{D}^{\text{corr}}$, which is identical except that the task-relevant information is removed. See Table 1 for a brief description and A for a long description of the individual tasks.

Metrics We quantify patching effects using the average logit difference (LD) over all samples for a given task. Let X^{clean} denote the correct answer for the clean input and let X^{corr} be the correct answer for the corrupted input. Let $L(X^{\text{clean}}, X^{\text{corr}}) = \text{Logit}(X^{\text{clean}}) - \text{Logit}(X^{\text{corr}})$. Logit difference is then defined as $L^*(X^{\text{clean}}, X^{\text{corr}}) - L'(X^{\text{clean}}, X^{\text{corr}})$ where L^* and L' denote logits from the patched and the corrupted runs. A positive score means that the model predicts the correct answer with a higher probability than the incorrect answer. Different LD implementations for various tasks are discussed in the Appendix A. In addition to using LD as our measure for circuit inclusion, we use

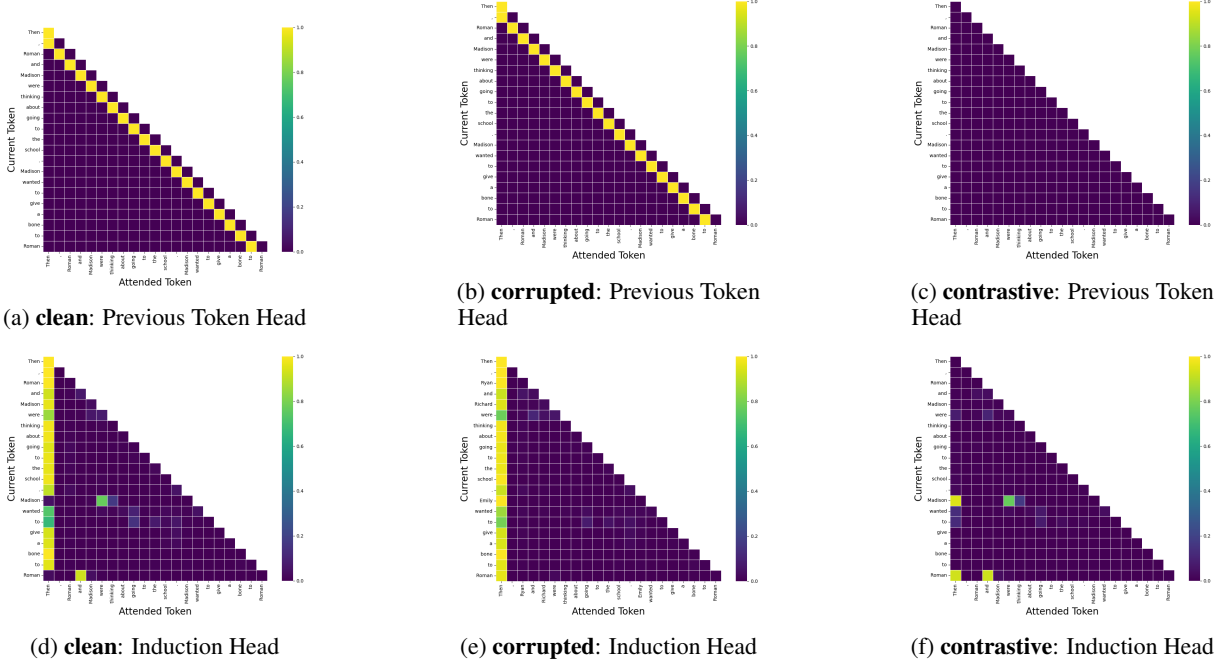


Figure 2: Activation Patterns of context-insensitive (**top**) and context-sensitive (**bottom**) heads. **Left:** clean activations, **middle:** corrupted activations, **right:** contrastive activations.

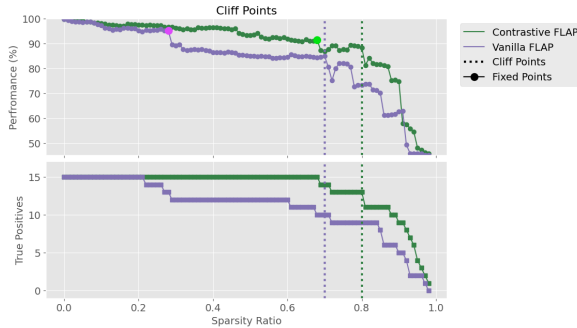


Figure 3: Performance and TP over a sparsity of 0 to 1 for vanilla and contrastive FLAP. Points are the fixed sparsity used in Table 2, dotted lines are the sparsity ratios found via cliff points.

average LD to measure the patching effect during PP and circuit performance. To evaluate circuit performance, all heads in the model, except for the ones included in the circuit are set to the corrupted activations. Performance is measured by the percentage of the original, average LD restored by the patched model.

3.2 Circuit Discovery with Path Patching

Activation patching and causal mediation analysis using contrastive minimal pairs form the basis for many circuit discovery methods. Activation patching measures the causal influence of model components by replacing their activations with cor-

rupted ones and comparing the resulting output. Path Patching (PP) (Wang et al., 2022; Goldowsky-Dill et al., 2023a) extends this idea by tracing information flow along specific computational paths. A path is defined by a sender node p and a receiver node r . During a forward pass on the clean dataset, \mathcal{D}^{clean} , activations at p are replaced with those from the corrupt dataset, \mathcal{D}^{corr} . A large logit difference between the patched and unpatched runs indicates that p causally affects r . PP is applied iteratively, starting from the final logits as receivers and all attention heads as senders. Heads with a causal effect become the new receivers, and earlier heads become senders. In this study, we apply PP only to attention heads and exclude MLPs. To reduce the manual effort required for circuit discovery, we use an iterative version of PP proposed by Zhang and Nanda (2024), which determines inclusion criteria based on the standard deviation of the average patching effect, referred to as Automatic PP. We further adapt this procedure using two thresholding criteria to determine circuit inclusion: the importance threshold and the maximum value threshold. First, the **importance threshold** is evaluated over each logit difference score $x_{i,j}$

$$|x_{i,j}| - |\bar{X}| > K * \text{SD}(X)$$

where \bar{X} and $\text{SD}(X)$ denote the mean and standard deviation calculated over all logit differences

respectively, and K is a predefined constant. At early layers in the model, the constant is adjusted to

$$K' = K + \frac{2}{\sqrt{l_s * H}}$$

where K' increases as l_s decreases. The adjusted constant K' is evaluated for each sender layer l_s . This adjustment ensures that path patching focuses on sequential influence: components that are more distant from the receiver must meet stricter significance criteria to be included. For evaluation, K is set to [1, 1.5, 2, 2.5]. The second criterion, **maximum value thresholds**, ensures that at least one score $x_{i,j}$ is above a chosen value ϵ . Otherwise, no head for the current receiver will be included in the circuit. This prevents the inclusion of spurious or weakly contributing components in the constructed circuit. Values chosen for ϵ are [0.01, 0.001, 0.02, 0.002]

Heads that exceed both threshold are considered significant contributors to the model’s behavior and are selected as receivers in subsequent iterations of the algorithm. Further details on automated path patching and comparisons between manual and automatic PP are provided in Appendix C. Circuits discovered by Automatic PP serve as the ground truth for pruning comparisons.

3.3 Contrastive FLAP

Preserving context-sensitive, task-critical heads is necessary for discovering high-performing, minimal circuits. As discussed in Section B, context-sensitive heads produce different activations across clean and corrupted data, while context-insensitive heads remain constant. Figure 2 illustrates the activation patterns of an induction head in GPT-2 under clean and corrupted inputs, as well as the corresponding contrastive activations (clean - corrupted). Since FLAP is based purely on the weight and activation patterns, it is not guaranteed to preserve task-specific heads. In Appendix D.1.2, we show empirically that vanilla FLAP prunes task-specific, context-sensitive heads at higher sparsity ratios, leading to poor task performance. In order to preserve task-specific, context-sensitive heads, we propose Contrastive-FLAP. Contrastive-FLAP computes activation scores for both clean and corrupted inputs and derives final scores on the contrastive activations (clean – corrupted). This procedure effectively isolates task-specific heads, as context-insensitive heads exhibit near-identical ac-

tivation patterns across clean and corrupted conditions, yielding negligible importance scores.

Formally, let $X_{clean} \in \mathbb{R}^{(B \times S) \times C_{in}}$, be the input activation under the clean dataset, where B is the batch size, S is the sequence length and C_{in} is the dimension of the input channel. Likewise, the input activations obtained by the corrupted dataset is $X_{corr} \in \mathbb{R}^{(B \times S) \times C_{in}}$ and $W \in \mathbb{R}^{(C_{out} \times C_{in})}$ is the weight matrix. Then, the importance scores for Contrastive FLAP \tilde{S} are calculated by

$$\tilde{S} = |W_{i,j}| * \|X_{clean} - X_{corr}\|_2$$

. Figure 2 (c) and (f) visualize that contrastive activations allow us to retain context-sensitive heads while excluding context-insensitive ones. In Appendix D.1.2, we find that Contrastive FLAP indeed excludes task-critical heads only at higher sparsity compared to vanilla FLAP.

Determining Sparsity Ratios with Cliff Points

In typical pruning scenarios, a sparsity ratio is pre-defined by the user. To determine the appropriate level of sparsity for contrastive pruning, we automatically select the sparsity ratio based on identified **cliff points**. Cliff points indicate the removal of task-critical heads that are crucial for maintaining high-performance. Selecting a sparsity level just before the drop ensures these components remain in the circuit. Additionally, a minimal sparsity level is set to 0.6 for both circuits. Using 0.6 as the minimum, we then consider three different cliff points are considered for evaluation: the first drop after 0.6, the biggest drop in performance after 0.6, and a fixed maximal sparsity value of 0.75. In Figure 3, the first drop is visualized for vanilla and Contrastive-FLAP.

3.4 Can Pruning find Circuit Components?

To investigate whether pruning can find circuit components, we first need to discover ground truth circuits. In this section, we focus on only GPT-2 small since circuits are well studied with this model. Automated PP is evaluated over 100 random samples per task. Two hyperparameters are tested and from all resulting circuit, the smallest circuit with a performance of at least 75% accuracy is selected. If no circuit achieves 75% accuracy, we select the circuit that maximizes performance, while minimizing circuit size. Vanilla and contrastive FLAP are computed over 200 samples per task. Instead of fixing a specific sparsity value, sparsity is varied

between 0 and 1 in increments of 0.1. The smallest pruning circuit matching the performance of the path patching circuit is selected. Table 2 reports the performance, size, and the sparsity ratio of the vanilla and Contrastive FLAP. Circuit size is defined as the total amount of included attention heads, while sparsity ratio is defined as the percentage of the model excluded from the circuit. If the circuit matches in size and a high TPR value is reported, FLAP circuits are similar to PP circuits.

Table 2 shows that PP circuits are smaller than pruning circuits when performance is matched. The PP circuits are at least 47.62% smaller than the vanilla FLAP circuits and at least 4.17% smaller than contrastive FLAP. On average, vanilla FLAP retains 86.61% of the ground truth heads discovered with Path Patching while maintaining an average sparsity of 0.45, while contrastive FLAP retains 86.17% of the ground truth heads with an average sparsity of 0.68, indicating that Contrastive FLAP is better able to identify task-critical heads and remove task-irrelevant heads when compare to vanilla FLAP. For the Gendered Pronouns task, vanilla FLAP produces a much larger circuit (87 heads) than the ground truth, whereas Contrastive FLAP preserves only 38 heads while achieving higher accuracy (74.78% vs. 72.98% for vanilla FLAP). In this case, Contrastive FLAP maintains 100% of the heads contained in the ground truth, PP circuit. Interestingly, for the Docstring task, Contrastive FLAP yields a circuit that outperforms the Path Patching (PP) circuit in task performance despite having a lower TPR. This suggests that TPR alone is an insufficient metric for evaluating circuit overlap quality. Moreover, it indicates that the PP circuit may not represent a unique or minimal “gold-standard” circuit since alternative sub-networks can achieve comparable or even superior task performance.

Pruning cannot be used as an alternative for circuit discovery since the resulting circuits are too large and fail to satisfy the minimality constraint. More importantly, vanilla pruning identifies statistically important rather than causally relevant components, often removing context-dependent heads. While Table 2 demonstrates that Contrastive FLAP is better suited for identifying smaller circuits compared to FLAP, it still produces circuits that are too large compared to Path Patching. Further, the failure of pruning to replace path patching can be linked to how pruning overlooks the compositional structure of circuits and does not consider how

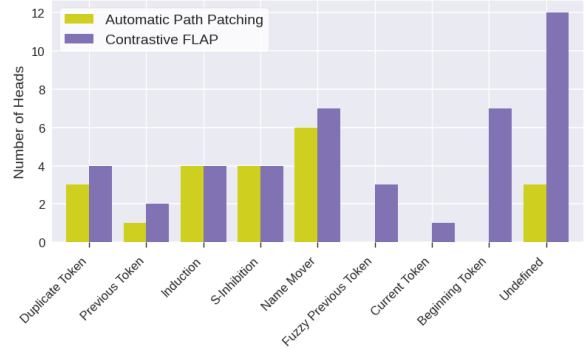


Figure 4: Comparison of attention head types identified by Contrastive FLAP and Automatic Path Patching for the IOI task in GPT-2 small.

multiple heads interact, whereas Path Patching explicitly isolates these causal pathways. Pruning can approximate task performance but cannot recover the causal and functionally minimal circuits revealed by mechanistic discovery methods. Instead of using pruning to replace Path Patching, we use both vanilla and Contrastive FLAP in tandem with circuit discovery methods to improve the efficiency of finding circuits.

4 Accelerated Path Patching (APP)

Despite the improvements of Contrastive FLAP, Figure 3 shows that while successfully preserving context-sensitive heads, some circuits depend on task-critical, yet context-insensitive heads that vanilla FLAP preserves. Further, in order to maintain similar performance to Path Patching, both vanilla FLAP and Contrastive-FLAP produce circuit sizes significantly larger than Path Patching, indicating that pruning does not satisfy the minimality constraint required for circuit analysis. Although pruning cannot be substituted for Path Patching since the resulting circuits, it can be used to *Accelerate* Path Patching by reducing the search space of circuit discovery algorithms. Specifically, Accelerated Path Patching (APP) follows a four-step process (See Figure 1):

1. Obtain a vanilla FLAP circuit using cliff points.
2. Obtain a Contrastive FLAP circuit using cliff points.
3. Merge the circuits found by the vanilla and Contrastive FLAP.
4. Apply Automated Path Patching on heads included in the merged FLAP circuit.

Model	Method	IOI			GreaterThan			GenderedPronouns			Induction			Docstring		
		Perf. (%)	Size (Sparsity)	TPR	Perf. (%)	Size (Sparsity)	TPR	Perf. (%)	Size (Sparsity)	TPR	Perf. (%)	Size (Sparsity)	TPR	Perf. (%)	Size (Sparsity)	TPR
GPT-2 Small	Path Patching	96.95	21 (0.85)	—	79.65	8 (0.94)	—	74.74	5 (0.97)	—	93.35	22 (0.83)	—	64.61	46 (0.68)	—
GPT-2 Small	FLAP	93.51	49 (0.66)	80.95	7.63	16 (0.89)	37.50	33.41	35 (0.76)	60.00	48.95	9 (0.94)	13.64	36.33	23 (0.84)	36.33
GPT-2 Small	Contrastive FLAP	67.34	22 (0.84)	76.19	69.38	31 (0.78)	87.50	32.44	29 (0.80)	80.00	89.39	45 (0.69)	90.91	69.39	52 (0.64)	71.73
GPT-2 Small	Merged	92.60	54 (0.63)	90.48	73.08	37 (0.74)	87.50	69.36	48 (0.67)	100.00	88.69	47 (0.67)	90.91	76.36	60 (0.58)	76.09
GPT-2 Large	Path Patching	92.60	193 (0.73)	—	75.71	27 (0.96)	—	73.94	73 (0.89)	—	90.90	67 (0.91)	—	73.19	122 (0.83)	—
GPT-2 Large	FLAP	69.97	186 (0.74)	46.11	106.90	186 (0.74)	74.07	68.15	244 (0.66)	67.12	41.57	107 (0.85)	35.82	75.27	201 (0.72)	56.56
GPT-2 Large	Contrastive FLAP	51.40	107 (0.85)	35.75	98.51	150 (0.79)	77.78	98.17	179 (0.75)	67.12	96.77	121 (0.83)	64.18	45.18	71 (0.90)	27.87
GPT-2 Large	Merged	86.85	220 (0.69)	53.37	105.28	237 (0.67)	85.19	96.20	310 (0.57)	82.19	99.25	186 (0.74)	71.16	84.05	221 (0.69)	61.48
Qwen2.5-0.5B	Path Patching	76.33	62 (0.82)	—	75.14	20 (0.94)	—	86.84	25 (0.93)	—	76.08	18 (0.95)	—	36.04	34 (0.90)	—
Qwen2.5-0.5B	FLAP	17.72	19 (0.94)	20.97	34.45	53 (0.84)	60.00	62.24	70 (0.79)	56.00	58.58	83 (0.75)	55.56	35.09	19 (0.94)	19.05
Qwen2.5-0.5B	Contrastive FLAP	82.84	113 (0.66)	67.74	87.01	130 (0.61)	95.00	55.27	59 (0.82)	40.00	93.12	127 (0.62)	100.00	72.13	133 (0.60)	85.71
Qwen2.5-0.5B	Merged	82.54	114 (0.66)	67.74	87.53	138 (0.59)	95.00	69.90	89 (0.74)	69.90	94.86	149 (0.56)	100.00	72.13	133 (0.60)	85.71
Qwen2.5-7B	Path Patching	73.25	221 (0.72)	—	79.33	34 (0.95)	—	68.69	125 (0.84)	—	67.90	10 (0.99)	—	64.79	150 (0.81)	—
Qwen2.5-7B	FLAP	9.38	195 (0.75)	41.17	30.29	195 (0.75)	52.94	2.02	195 (0.75)	41.60	77.46	148 (0.81)	50.00	36.45	195 (0.75)	47.33
Qwen2.5-7B	Contrastive FLAP	71.23	219 (0.72)	55.20	84.37	132 (0.83)	47.06	21.27	250 (0.68)	56.00	61.61	101 (0.87)	50.00	70.58	258 (0.67)	70.66
Qwen2.5-7B	Merged	82.09	303 (0.61)	74.38	88.03	232 (0.70)	67.65	70.92	317 (0.59)	61.60	93.03	206 (0.74)	60.00	73.57	336 (0.57)	79.33

Table 2: Comparison of performance, size, and true positive rate (TPR) between Path Patching, FLAP, Contrastive FLAP, and the merged circuits (FLAP + Contrastive FLAP).

By merging circuits from vanilla FLAP and Contrastive FLAP, we are able to find task-critical heads that are both context-sensitive and context-insensitive heads in order to preserve highly faithful circuits. Merging the circuits from Step 3 of APP still yields an average 56% reduction in attention heads and significantly reduces the overall runtime of circuit discovery algorithms. Note that while we apply automated Path Patching as the circuit discovery algorithm in Step 4 of APP, alternative circuit discovery methods that target attention heads as circuit components can be utilized with APP.

4.1 Efficient Circuit Discovery with APP

To demonstrate that APP scales to larger models, PP and APP are compared across the GPT-2 small, GPT-2 large, Qwen2.5-0.5B and Qwen2.5-7B model. If available, the smallest circuits with a performance of at least 75% is chosen in both cases. Both algorithms are executed on 100 random samples from all five tasks. In a preliminary experiment across all five tasks and four models (see Table 5), circuits for vanilla and Contrastive FLAP are identified via cliff points and merged to form Hybrid FLAP circuits. The resulting Hybrid FLAP circuit maintains a relatively high amount of ground truth heads across all models and tasks. The hybrid circuit reduces the search space by at least 56%. APP and automated PP are evaluated on two dimensions: accuracy and efficiency. For accuracy, we report performance, circuit size, sparsity, TPR, and precision (P). High TPR and precision indicate close alignment with the PP circuit. Efficiency is measured by required GFLOPs and computation time.

We first analyze the computational efficiency gains of APP over PP. Figure 5 visualizes the efficiency gains of APP (orange) compared to PP

(blue) in terms of GFLOPs. For the large models (GPT-2 large and Qwen2.5-7B) APP requires **4.11-14.87x less GFLOPs** than PP and GPT2-small and Qwen2.5-0.5B require **2.45-8.33 times less GFLOPs**. A similar pattern emerges for the required computation time (see Figure 8). The docstring task consistently requires the most FLOPs for both APP and PP, due to its larger discovered hybrid FLAP circuits, resulting in more PP iterations, and its longer input sequence length (52 tokens, compared to 21 for IOI, the second longest).

Despite the improved efficiency, Table 3 shows that APP circuits achieve an average performance of 70.42 with a sparsity ratio of 0.9, whereas PP produces circuits with higher performance (76.00) and a slightly lower sparsity ratio of 0.87. When comparing models, the highest average TPR (77.53%) is obtained with GPT-2 small and the highest average precision (86.22%) with the GPT-2 large model. The chosen set of hyperparameters is not optimal for GPT-2 large. For the IOI and induction task, APP misses some heads, therefor PP results in non-minimal circuits for the other tasks.

5 Conclusion and Discussion

Circuit discovery and pruning share the common goal of identifying subnetworks that replicate the full model’s behavior on downstream tasks. In this study, we first examine whether highly efficient pruning can provide a faster, more computationally efficient alternative to Path Patching. We find that circuits identified through pruning are substantially larger than those obtained via Path Patching, suggesting that pruning alone is insufficient for circuit discovery, as it fails to satisfy the minimality constraints required by circuit analysis. The inability to find minimal circuits is reflected in the limitations of current pruning algorithms at high sparsity

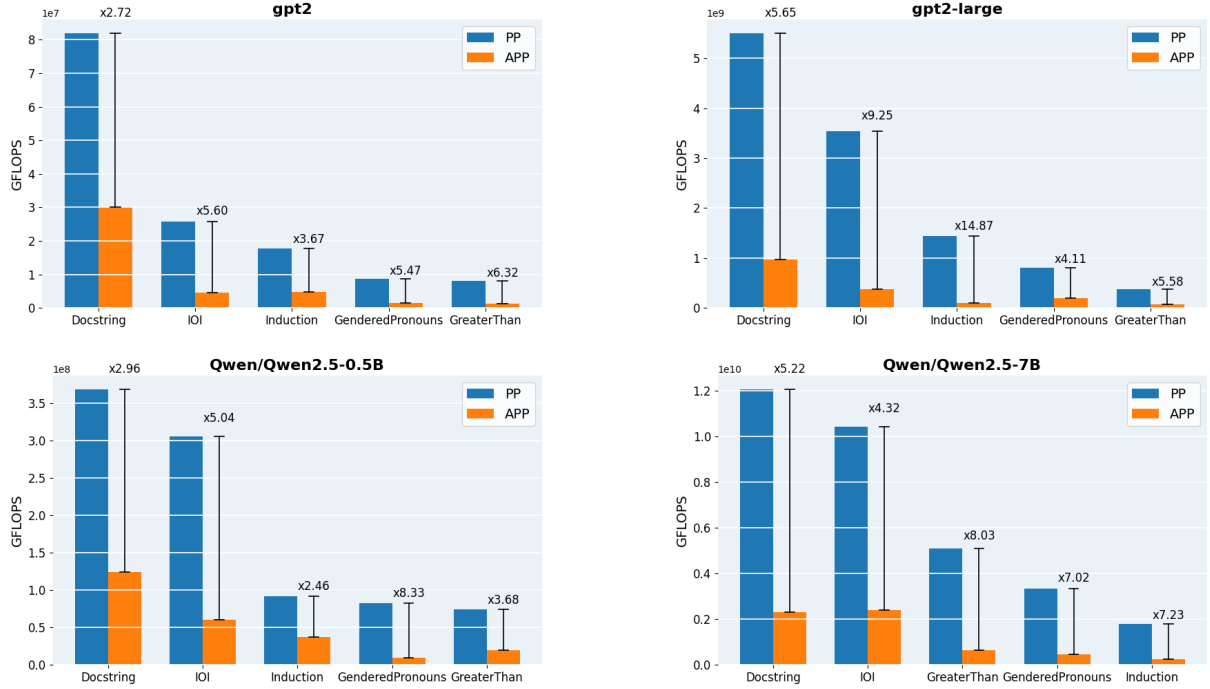


Figure 5: Difference of required GFLOPs across all models and tasks

Model	Method	IOI			GreaterThan			GenderedPronouns			Induction			Docstring				
		Perf. (%)	Size	TPR	P	Perf. (%)	Size	TPR	P	Perf. (%)	Size	TPR	P	Perf. (%)	Size	TPR	P	
GPT-2 small	PP	96.95	21 (0.85)	-	-	79.65	8 (0.94)	-	-	74.74	5 (0.97)	-	-	93.35	22 (0.83)	-	-	
	APP	82.47	19 (0.87)	85.71	94.73	76.71	18 (0.88)	87.5	38.89	74.61	5 (0.97)	80.0	80.0	90.35	16 (0.88)	68.18	93.35	56.21
GPT-2 large	PP	92.60	193 (0.73)	-	-	75.71	27 (0.96)	-	-	73.94	73 (0.89)	-	-	90.90	67 (0.91)	-	-	
	APP	68.33	92 (0.87)	47.66	100.0	76.89	23 (0.97)	77.78	91.30	79.65	23 (0.97)	34.24	100.0	84.14	87 (0.88)	58.21	44.82	54.36
Qwen2.5-0.5B	PP	76.33	62 (0.82)	-	-	75.14	20 (0.94)	-	-	86.84	25 (0.93)	-	-	76.08	18 (0.95)	-	-	
	APP	76.26	36 (0.89)	56.45	97.22	75.05	28 (0.92)	80.0	57.14	60.83	33 (0.90)	44.0	33.33	84.20	21 (0.94)	83.33	71.43	36.63
Qwen2.5-7B	PP	61.06	121 (0.85)	-	-	79.33	34 (0.95)	-	-	68.69	125 (0.84)	-	-	67.90	10 (0.99)	-	-	
	APP	61.87	137 (0.83)	74.38	53.57	79.43	62 (0.92)	67.65	37.10	76.88	126 (0.84)	48.0	47.62	64.98	6 (0.99)	40.0	66.67	48.68
Average	PP	84.78	0.78	-	-	77.46	0.95	-	-	76.05	0.91	-	-	82.06	0.92	-	-	
Average	APP	72.23	0.87	66.06	86.38	77.02	0.92	78.23	56.11	72.99	0.92	51.56	65.24	80.92	0.92	62.43	69.07	48.96

Table 3: Compare the APP and PP method based on their performance (Perf), size (and sparsity), recall (TPR) and precision (P).

levels, with models often experiencing catastrophic performance degradation when pruned beyond 70% (Beck et al., 2025). Further, we find that even at lower sparsity ratios, methods such as FLAP often prune critical context-sensitive attention heads, such as induction heads that are required for tasks such as IOI.

We posit that this is largely due to the pruning decision in FLAP being based solely on weights and activations. A high importance score for an attention head does not necessarily imply that the head is critical for solving the task. For instance, Liu and Liu (2025) claims that the position of an attention head is an important factor to identify critical attention heads, not only the attention score. In order to better preserve context-sensitive heads, we propose Contrastive FLAP, which calculates importance scores on the activation differences of contrastive pairs. Contrastive FLAP is able to achieve

a significantly sparser model for the same performance as vanilla FLAP, indicating that Contrastive FLAP is a promising standalone pruning method. Figure 4 demonstrates that Contrastive FLAP identifies all head types but also includes undefined, task-agnostic heads, indicating that, despite its improvements, Contrastive FLAP alone cannot serve as a replacement for circuit discovery methods.

Although pruning alone cannot replace Path Patching due to the large circuits it produces, Table 2 shows that it achieves a high recall of Path Patching circuits. Building on this, we introduce Accelerated Path Patching (APP), which uses Contrastive-FLAP to reduce the search space before applying any circuit discovery algorithm. APP maintains high task performance while substantially improving efficiency, enabling circuit discovery methods to scale to larger models. Table 3 illustrates that APP can achieve high precision even

when TPR is low, indicating that it successfully removes redundant heads and identifies more compact circuits. In other cases, high TPR with lower precision suggests that minimal circuits remain elusive. Overall, despite the significant gains in computational efficiency, APP often produces circuits of similar size and performance compared to Path Patching. By serving as a general preprocessing step, APP makes any circuit discovery method faster and more practical, offering a scalable path toward efficient mechanistic interpretability.

6 Limitations

Table 3 shows that neither automated PP nor APP consistently yields optimal circuits in terms of minimality and performance. One reason is that the hyperparameter search is limited by the computational cost of PP on large models like Qwen2.5-7B. Exploring a wider range of hyperparameters solely on APP could find better circuits across all models and tasks. Another challenge is deciding the best trade-off between circuit size and performance. While curve fitting or Pareto analysis can help, the final decision remains the responsibility of the researcher. Furthermore, the ability of APP to retrieve the same circuits as PP is capped by the TPR of hybrid FLAP. If the hybrid FLAP circuit is too small, APP will not recover all heads. Our work focuses on circuit discovery and not circuit analysis. To the best of our knowledge, except for GPT-2 small, path patching has not been applied to the here tested large models, and thus comparison to other work is not possible. Studying whether circuits discovered in GPT-2 small translate to larger models, or if new behavior arises, would be very interesting. APP, as proposed here, focuses on attention heads, since various related works in mechanistic interpretability make the same choice. Nonetheless, some natural language tasks, such as factual association (Meng et al., 2022a), rely heavily on the MLP components. Since FLAP supports MLP patching, these components could be incorporated into the automated path patching method if desired. The heuristic of reducing the search space via pruning is not limited to PP. Other algorithms, such as ACDC could be enhanced in the same way, but this is left for future work.

7 Acknowledgments

This work was supported by the National Science Foundation under Cooperative Agreement

2421782 and the Simons Foundation award MPS-AI-00010515 (NSF-Simons AI Institute for Cosmic Origins - CosmicAI, <https://www.cosmicai.org/>)

References

- Yongqi An, Xu Zhao, Tao Yu, Ming Tang, and Jinqiao Wang. 2024. [Fluctuation-based adaptive structured pruning for large language models](#). *Proceedings of the AAAI Conference on Artificial Intelligence*, 38(10):10865–10873.
- Florentin Beck, William Rudman, and Carsten Eickhoff. 2025. [Trim: Achieving extreme sparsity with targeted row-wise iterative metric-driven pruning](#). *Preprint*, arXiv:2505.16743.
- Arthur Conmy, Augustine N. Mavor-Parker, Aengus Lynch, Stefan Heimersheim, and Adrià Garriga-Alonso. 2023. [Towards automated circuit discovery for mechanistic interpretability](#). *Preprint*, arXiv:2304.14997.
- Nelson Elhage, Neel Nanda, Catherine Olsson, Tom Henighan, Nicholas Joseph, Ben Mann, Amanda Askell, Yuntao Bai, Anna Chen, Tom Conerly, and 1 others. 2021. [A mathematical framework for transformer circuits](#). *Transformer Circuits Thread*, 1(1):12.
- Angela Fan, Edouard Grave, and Armand Joulin. 2019. [Reducing transformer depth on demand with structured dropout](#). *Preprint*, arXiv:1909.11556.
- Jonathan Frankle and Michael Carbin. 2018. [The lottery ticket hypothesis: Finding sparse, trainable neural networks](#). *arXiv: Learning*.
- Elias Frantar and Dan Alistarh. 2023. [SparseGPT: Massive language models can be accurately pruned in one-shot](#). In *Proceedings of the 40th International Conference on Machine Learning*, volume 202 of *Proceedings of Machine Learning Research*, pages 10323–10337. PMLR.
- Atticus Geiger, Hanson Lu, Thomas F. Icard, and Christopher Potts. 2021. [Causal abstractions of neural networks](#). In *Neural Information Processing Systems*.
- Nicholas Goldowsky-Dill, Chris MacLeod, Lucas Sato, and Aryaman Arora. 2023a. [Localizing model behavior with path patching](#). *Preprint*, arXiv:2304.05969.
- Nicholas Goldowsky-Dill, Chris MacLeod, Lucas Sato, and Aryaman Arora. 2023b. [Localizing model behavior with path patching](#). *Preprint*, arXiv:2304.05969.
- Michal Golovanevsky, William Rudman, Vedant Palit, Ritambhara Singh, and Carsten Eickhoff. 2025. [What do vlms notice? a mechanistic interpretability pipeline for gaussian-noise-free text-image corruption and evaluation](#). *Preprint*, arXiv:2406.16320.

- Michael Hanna, Ollie Liu, and Alexandre Variengien. 2023. *How does gpt-2 compute greater-than?: Interpreting mathematical abilities in a pre-trained language model*. In *Advances in Neural Information Processing Systems*, volume 36, pages 76033–76060. Curran Associates, Inc.
- Michael Hanna, Sandro Pezzelle, and Yonatan Belinkov. 2024. *Have faith in faithfulness: Going beyond circuit overlap when finding model mechanisms*. In *ICML 2024 Workshop on Mechanistic Interpretability*.
- Stefan Heimersheim and Jett Janiak. *A circuit for python docstrings in a 4-layer attention-only*.
- Songtao Liu and Peng Liu. 2025. *High-layer attention pruning with rescaling*. *Preprint*, arXiv:2507.01900.
- Xinyin Ma, Gongfan Fang, and Xinchao Wang. 2023. *Llm-pruner: On the structural pruning of large language models*. In *Advances in Neural Information Processing Systems*, volume 36, pages 21702–21720. Curran Associates, Inc.
- Chris Mathwin, Guillaume Corlouer, Esben Kran, Fazl Barez, and Neel Nanda. 2023. Identifying a preliminary circuit for predicting gendered pronouns in gpt-2 small. URL: <https://itch.io/jam/mechint/rate/1889871>.
- Kevin Meng, David Bau, Alex Andonian, and Yonatan Belinkov. 2022a. *Locating and editing factual associations in gpt*. In *Advances in Neural Information Processing Systems*, volume 35, pages 17359–17372. Curran Associates, Inc.
- Kevin Meng, David Bau, Alex Andonian, and Yonatan Belinkov. 2022b. Locating and editing factual associations in GPT. *Advances in Neural Information Processing Systems*, 36. ArXiv:2202.05262.
- Nostalgebraist. 2020. *Interpreting gpt: the logit lens*.
- Chris Olah. 2022. Mechanistic interpretability, variables, and the importance of interpretable bases. <https://www.transformer-circuits.pub/2022/mech-interp-essay>. Published June 27, 2022; Accessed: 2025-10-02.
- Chris Olah, Nick Cammarata, Ludwig Schubert, Gabriel Goh, Michael Petrov, and Shan Carter. 2020. *Zoom in: An introduction to circuits*. *Distill*. <Https://distill.pub/2020/circuits/zoom-in>.
- Alec Radford, Jeff Wu, Rewon Child, David Luan, Dario Amodei, and Ilya Sutskever. 2019. *Language models are unsupervised multitask learners*.
- E Rutherford. 1905. Xxxvii. slow transformation products of radium. *The London, Edinburgh, and Dublin Philosophical Magazine and Journal of Science*, 10(57):290–306.
- Mingjie Sun, Zhuang Liu, Anna Bair, and J. Zico Kolter. 2024. *A simple and effective pruning approach for large language models*. *Preprint*, arXiv:2306.11695.
- Aaquib Syed, Can Rager, and Arthur Conmy. 2023. *Attribution patching outperforms automated circuit discovery*. *Preprint*, arXiv:2310.10348.
- Jesse Vig, Sebastian Gehrmann, Yonatan Belinkov, Sharon Qian, Daniel Nevo, Simas Sakenis, Jason Huang, Yaron Singer, and Stuart Shieber. 2020. *Causal mediation analysis for interpreting neural nlp: The case of gender bias*. *Preprint*, arXiv:2004.12265.
- Kevin Wang, Alexandre Variengien, Arthur Conmy, Buck Shlegeris, and Jacob Steinhardt. 2022. *Interpretability in the wild: a circuit for indirect object identification in gpt-2 small*. *Preprint*, arXiv:2211.00593.
- Qwen An Yang, Baosong Yang, Beichen Zhang, Binyuan Hui, Bo Zheng, Bowen Yu, Chengyuan Li, Dayiheng Liu, Fei Huang, Guanting Dong, Haoran Wei, Huan Lin, Jian Yang, Jianhong Tu, Jianwei Zhang, Jianxin Yang, Jiaxin Yang, Jingren Zhou, Junyang Lin, and 25 others. 2024. *Qwen2.5 technical report*. *ArXiv*, abs/2412.15115.
- Qinan Yu, Jack Merullo, and Ellie Pavlick. 2023. *Characterizing mechanisms for factual recall in language models*. *ArXiv*, abs/2310.15910.
- Fred Zhang and Neel Nanda. 2024. *Towards best practices of activation patching in language models: Metrics and methods*. *Preprint*, arXiv:2309.16042.
- Ruochen Zhang, Qinan Yu, Matianyu Zang, Carsten Eickhoff, and Ellie Pavlick. 2024. *The same but different: Structural similarities and differences in multilingual language modeling*. *ArXiv*, abs/2410.09223.
- Xunyu Zhu, Jian Li, Yong Liu, Can Ma, and Weiping Wang. 2024. *A survey on model compression for large language models*. *Transactions of the Association for Computational Linguistics*, 12:1556–1577.

A Tasks

A.1 IOI Task

The IOI task (Wang et al., 2022) evaluates whether a model can correctly predict the indirect object in a sentence. For example, a clean prompt is “*When John and Mary went to the store, John bought a drink for...*”. John is the subject of the sentence and the correct continuation; “*Mary*” is the indirect object. A corrupted prompt removes the semantic cue from the indirect object, for example, “*When John and Mary went to the store, Alex bought a drink for...*”.

Task performance is measured using the logit difference, defined as the logit of the indirect object minus the logit of the subject. In the example above:

$$\text{LD} = \text{Logit}(\text{Mary}) - \text{Logit}(\text{John})$$

We use the implementation of the IOI dataset from the ARENA tutorial repository³. The corrupted dataset is generated using the "ABB→XYZ, BAB→XYZ" command.

A.2 GreaterThan Task

The objective of the GreaterThan task (Hanna et al., 2023) is to evaluate the model’s ability to predict a number greater than another within a natural language context. The template is: "*The <NOUN> lasted from XXYY to the year XX..*", where $XX \in \{11, \dots, 17\}$ and $YY \in \{02, \dots, 98\}$. The model is supposed to predict a number $\geq YY$. The corrupted prompt is of the form: "*The <NOUN> lasted from XX01 to the year XX..*".

The tokenizer of the GPT family encodes YY as [YY], and it predicts answer v as one token. Thus, the logit difference is as follows.

$$\text{Correct} = \{v | (v > YY) \wedge (v \leq 98)\}$$

$$\text{Wrong} = \{v | v \leq YY\}$$

$$\text{LD} = \text{Logits(Correct)} - \text{Logits(Wrong)}$$

The Qwen2.5 tokenizer encodes YY in two tokens [Y₁][Y₂]. The predicted answer is tokenized in the same manner [v₁][v₂]. With $Y_1, Y_2, v_1, v_2 = 0, \dots, 9$ Hence the average logit difference is

$$\text{Correct} =$$

$$\{v_1v_2 | (v_1 > Y_1) \vee (v_1 = Y_1 \wedge v_2 > Y_2)\}$$

$$\text{Wrong} =$$

$$\{v_1v_2 | (v_1 < Y_1) \vee (v_1 = Y_1 \wedge v_2 \leq Y_2)\}$$

$$\text{LD} = \text{Logits(Correct)} - \text{Logits(Wrong)}$$

The GreaterThan Dataset is downloaded from the original HuggingFace data repo⁴.

A.3 GenderedPronouns Task

The GenderedPronouns Task (Mathwin et al., 2023) evaluates a model’s ability to predict the pronoun conventionally associated with a gendered name. While exceptions to these associations exist, we adopt this simplification for clarity.

A clean sample from the dataset is "*So Emily is such a good friend, isn’t...*" with the correct answer *she*. The corresponding corrupted prompt replaces

³https://github.com/callummcdougall/ARENA_3.0/blob/main/chapter1_transformer_interp/exercises/part41_indirect_object_identification/loi_dataset.py

⁴<https://huggingface.co/datasets/mwhanna/greater-than>

the gendered name with a non-gendered description: "*That person is such a good friend, isn’t...*". The clean prompt begins with the filler word "So" to preserve grammatical cohesion in the corrupted version, while maintaining structural equivalence between the two prompts. Without "So", the corrupted prompt would be one token longer, requiring the removal of "That" in the corrupted prompt.

The average logit difference is calculated by the difference between the correct pronoun and the wrong pronoun for the name. In the given example, that is $\text{LD} = \text{Logits}(\text{she}) - \text{Logits}(\text{he})$.

A.4 Induction Task

The induction task uses token sequences of the form [A][B]...[A], where the model’s objective is to predict [B] as the next token. Our implementation differs from Goldowsky-Dill et al. (2023b), by focusing on name induction. For example, a clean prompt has the following form: "*Today, Claire visited the library. There Cl...*". The correct next prediction is "*aire*". The corrupted prompt replaces the repeated name with another, e.g. "*Today, Claire visited the library. There Tr...*". It is important that only names that the tokenizer splits into exactly two tokens [Name₁][Name₂] are used.

The average logit difference is defined as the difference between the logits of the second token of the correct name and the second token of the corrupted name: $\text{LD} = \text{Logits}(\text{aire}) - \text{Logits}(\text{istan})$.

A.5 Docstring Task

The docstring task (Heimersheim and Janiak) evaluates a model’s ability to complete a Python Docstring. A clean prompt has the following form:

```
DEF OLD(SELF, FIRST, PAGE, NAMES, SIZE,
FILES, READ):
    """sector gap population
:param page: message tree
:param names: detail mine
:param ..."""

```

The correct next token is SIZE. The corresponding corrupted prompt is the following.

```
DEF OLD(SELF, FIRST, PROJECT, TARGET,
NEW, FILES, READ):
    """sector gap population
:param image: message tree
:param update: detail mine
:param ..."""

```

The logit difference is the difference between the logits of the correct answer and max logit of all

wrong variables of the clean and corrupted prompt.

```
Wrong =
{first, page, names, files, read, project, target, new}
LD = Logits(size) - arg max Logits(x)

$$x \in \text{Wrong}$$

```

The code for the dataset is taken from this repository⁵.

B Context Sensitive vs. Task-Critical Heads

Context-Sensitive Attention Heads Meng et al. (2022b) identify various types of attention heads for the IOI task in the GPT-2 small model. For example, the *Previous Token Heads* always attend to the token immediately preceding the current one. These heads exhibit the same activation pattern regardless of the provided input and are therefore called **context-insensitive**. Figure 2 visualizes the activation pattern of a previous token head on the clean (a) and corrupted (b) dataset. Although the token input of the two datasets differs, the observed activation pattern is the same.

Conversely, heads that display a distinct activation pattern only when a specific token pattern is present, are **context-sensitive**. For example, an *Induction Head* strongly attends to the token [B] when it encounters the token sequence [A][B] ... [A]. By definition, context-sensitive heads should remain inactive on samples from the corrupted dataset, because the token pattern is not detected (see Figure 2, (d) + (e)). Note that context-sensitive heads are activated only by specific token context, whereas task-critical heads are defined as essential for solving a task and are ideally included in the corresponding circuit. Many, but not all, task-critical heads are context-sensitive (e.g. previous token heads).

C Automatic Path Patching

C.1 Implementation

The procedure to automate path patching is summarized in Algorithm 1 and is heavily inspired by Zhang and Nanda (2024). PATHPATCHING encodes the standard path patching mechanism introduced by Wang et al. (2022). In the EVALUATETHRESHOLD function, two thresholds are decided based on a head-wise influence score to determine whether an attention head is included in the circuit.

⁵https://github.com/jettjaniak/mi_utils_public/blob/main/prompts.py

Algorithm 1: Automatic Path Patching

Result: circuit

```

1 circuit ← {}
2 influenceScores ← PathPatching (logits)
    // influenceScores ∈ ℝ(L × H)
3 receiverList ← EvaluateThresholds
    (influenceScores)
4 while receiverList not empty do
5     receiver ← pop(receiverList)
        // layer l, head h
6     circuit.add(receiver)
7     influenceScores ← PathPatching
        (receiver) // influenceScores
        ∈ ℝ((l-1) × H)
8     senderList ← EvaluateThresholds
        (influenceScores)
9     for s in senderList do
10        if s not in receiverList & s not in
            circuit then
11            receiverList.add(s)
12        end
13    end
14 end
```

To discuss the threshold, we will first provide some notations. Assume that the total number of layers of a model is L and that each layer contains H attention heads. A receiver head r can be defined by the tuple $r = (l_r, h_r)$, where $l_r \leq L$ and $h_r \leq H$. Sender heads are denoted as $s = (l_s, h_s)$ and correspond to all heads from earlier layers ($l_s < l_r$) that patch to r . The influence of patching a head from earlier layers is measured by an influence score, typically the *average logit difference*. The influence scores of all previous heads are collected in the matrix $X \in \mathbb{R}^{(l_r-1) \times H}$.

First, the **importance threshold** is evaluated over each importance score $x_{i,j}$

$$|x_{i,j}| - |\bar{X}| > K * \text{SD}(X)$$

, where \bar{X} and $\text{SD}(X)$ denote the mean and standard deviation calculated over all influence scores respectively, and K is a predefined constant. At lower-level layers, the scores become noisier. To account for this, the constant is adjusted to

$$K' = K + \frac{2}{\sqrt{l_s * H}}$$

, where K' increases as l_s decreases. The adjusted constant K' is evaluated for each sender layer l_s .

This adjustment is desirable, since path patching focuses on sequential influence: components that are more distant from the receiver must meet stricter significance criteria to be included. For evaluation, K is set to [1, 1.5, 2, 2.5].

Second, the **maximum value thresholds** ensure that at least one score $x_{i,j}$ is above a chosen value ϵ . Otherwise, no head for the current receiver will be included in the circuit. This prevents the inclusion of spurious or weakly contributing components in the constructed circuit. Values chosen for ϵ are [0.01, 0.001, 0.02, 0.002]

Heads that exceed both thresholds are considered significant contributors to the model’s behavior and are selected as receivers in subsequent iterations of the algorithm.

D Pruning

D.1 Implementation of Vanilla FLAP

Since FLAP (An et al., 2024) is a zero-shot pruning algorithm that utilizes head-wise importance scores and does not require retraining it is possible to have a direct comparison with path patching. The influence scores are calculated by passing samples of the dataset \mathcal{D}_{clean} to the FLAP algorithm. Based on a sparsity level p , the $1 - p\%$ heads with the highest importance score are chosen to be in the circuit. By design, heads that yield in higher importance scores have higher weights and/or input activation values during the forward pass. Theoretically, these higher values translate to a higher influence on the output logits. Thus, these heads are likely to have a stronger influence on the next prediction and are considered to be in the circuit.

Since FLAP is computationally very efficient, it can be run on multiple times to evaluate the performance of the resulting circuits under different sparsity levels.

D.1.1 Implementation of Contrastive FLAP

Contrastive FLAP is summarized in Algorithm 4. The method computes FLAP scores for both clean and corrupted inputs, then evaluates the absolute difference between the two. Attention heads are subsequently ranked globally according to their contrastive FLAP scores, and the top $s\%$ with the highest ratios are selected and incorporated into the circuit.

Algorithm 2: Contrastive FLAP

Result: circuit

```

1 FLAPScores ←
    calculateImportanceScore
    (cleanDataset)
2 corruptedFLAPScores ←
    calculateImportanceScore
    (corruptedDataset)
3 contrastiveFLAPScores
    ← ||FLAPScores-
        corruptedFLAPScores ||
4 circuit ←
    pruneHeads(contrastiveFLAPScores,
    sparsityRatio);

```

D.1.2 Does Contrastive FLAP find smaller circuits than vanilla FLAP?

Methods Contrastive and Vanilla FLAP are evaluated on the GPT-2 small model for all five tasks presented in 2. Each task had a clean and corrupted dataset with 200 randomly picked samples.

Metric The **half-life** metric ($t_{\frac{1}{2}}$), originally used to quantify the exponential nature of radioactive decay (Rutherford, 1905), measures the time required for a quantity to reach half of its initial value. Here, the metric is applied to the total number of true positive heads, with sparsity levels ranging from 0 to 1 in increments of 0.01 serving as the analog of time. A higher half-life value translates to a later exclusion of critical heads and thus an earlier exclusion of task-irrelevant heads.

Results Except for the IOI task, the half-life value is reached only at higher sparsity levels for circuits identified by contrastive FLAP (see Table 7). This indicates that 50% of the ground truth heads are removed at higher sparsity levels. Figure 6 visualizes the exclusion of ground truth heads across all tested sparsity levels. contrastive FLAP maintains a plateau longer at lower sparsity compared to Vanilla FLAP. This effect is particularly pronounced for the Induction task, where the first exclusion of a ground truth head occurs at a sparsity level of 0.57, compared to 0.13 for Vanilla FLAP. A similar trend is observed for the IOI task. On the other hand, the two curves for the GreaterThan task are nearly identical, suggesting that some tasks benefit more

	IOI		GreaterThan		GenderedPronouns		Induction		Docstring	
	Manual	Automatic	Manual	Automatic	Manual	Automatic	Manual	Automatic	Manual	Automatic
Perf. (%)	75.58	96.95	71.68	79.65	80.16	74.74	86.34	93.35	41.06	60.36
Size	15	21	8	8	7	5	14	22	23	36
Intersection	-	14	-	6	-	4	-	13	-	22
Difference	-	7	-	2	-	1	-	9	-	14

Table 4: Circuits discovered by manual and automatic path patching on GPT-2 small

D.1.3 Hybrid FLAP

Methods Circuits of all three methods are evaluated over 200 samples for all five tasks and all three cliff points. See Appendix E to see which circuit was chosen for each task. Since the goal is to scale path patching to larger models, GPT-2 small, GPT-2 large, Qwen2.5-0.5B and Qwen2.5-7B are evaluated. See Appendix C to see results for the automatic path patching algorithms for all models. Circuits for Hybrid FLAP are chosen by evaluating all possible combinations of cliff points from contrastive and vanilla FLAP. The one with the best trade-off between performance and size is chosen.

Results Hybrid FLAP yields in circuits with an average TPR of 82.39% for GPT-2 small, 68.12% for GPT-2 large, 80.07% for Qwen2.5-0.5B and 73.73% for Qwen2.5-7B (see Table 5). With a minimum sparsity ratio of 0.58 for the Docstring task on GPT-2 small, 0.64 for the GreaterThan task for GPT-2 large, 0.56 for the Induction task on Qwen2.5-0.5B and 0.57 for the Docstring task on Qwen2.5-7B. Altough Hybrid FLAP circuits are larger than the ones discovered by Vanilla or contrastive FLAP, the TPR is higher and performance are generally higher.

E Accelerated Path Patching: Efficiency

The efficiency gains in terms of computation time paint a similar pattern to the GFLOPs. APP yields a significant speed-up compared to PP (see Figure 8).

F Hyperparameters Tuning

F.1 Automatic Path Patching

In Figure 9, 10, 11, and 12, we show the resulting circuits from Automatic PP and model performances across tasks and model families under different hyperparameter settings.

F.2 Accelerated Path Patching

In Figure 13, 14, 15, and 16, we show the resulting circuits from APP and model performances across tasks and model families under different hyperparameter settings.

Model	FLAP Method	IOI			GreaterThan			GenderedPronouns			Induction			Docstring		
		Perf. (%)	Size (Sparsity)	TPR	Perf. (%)	Size (Sparsity)	TPR	Perf. (%)	Size (Sparsity)	TPR	Perf. (%)	Size (Sparsity)	TPR	Perf. (%)	Size (Sparsity)	TPR
GPT-2 small	Path Patching	96.95	21 (0.85)	-	79.65	8 (0.94)	-	74.74	5 (0.97)	-	93.35	22 (0.83)	-	64.61	46 (0.68)	-
GPT-2 small	Clean	93.51	49 (0.66)	80.95	7.63	16 (0.89)	37.50	33.41	35 (0.76)	60.00	48.95	9 (0.94)	13.64	36.33	23 (0.84)	36.33
GPT-2 small	Contrastive	67.34	22 (0.84)	76.19	69.38	31 (0.78)	87.50	32.44	29 (0.80)	80.00	89.39	45 (0.69)	90.91	69.39	52 (0.64)	71.73
GPT-2 small	Merged	92.60	54 (0.63)	90.48	73.08	37 (0.74)	87.50	69.36	48 (0.67)	100.00	88.69	47 (0.67)	90.91	76.36	60 (0.58)	76.09
GPT-2 large	Path Patching	92.60	193 (0.73)	-	75.71	27 (0.96)	-	73.94	73 (0.89)	-	90.90	67 (0.91)	-	73.19	122 (0.83)	-
GPT-2 large	Clean	69.97	186 (0.74)	46.11	106.90	186 (0.74)	74.07	68.15	244 (0.66)	67.12	41.57	107 (0.85)	35.82	75.27	201 (0.72)	56.56
GPT-2 large	Contrastive	51.40	107 (0.85)	35.75	98.51	150 (0.79)	77.78	98.17	179 (0.75)	67.12	96.77	121 (0.83)	64.18	45.18	71 (0.90)	27.87
GPT-2 large	Merged	86.85	220 (0.69)	53.37	105.28	237 (0.67)	85.19	96.20	310 (0.57)	82.19	99.25	186 (0.74)	71.16	84.05	221 (0.69)	61.48
Qwen2.5-0.5B	Path Patching	76.33	62 (0.82)	-	75.14	20 (0.94)	-	86.84	25 (0.93)	-	76.08	18 (0.95)	-	36.04	34 (0.90)	-
Qwen2.5-0.5B	Clean	17.72	19 (0.94)	20.97	34.45	53 (0.84)	60.00	62.24	70 (0.79)	56.00	58.58	83 (0.75)	55.56	35.09	19 (0.94)	19.05
Qwen2.5-0.5B	Contrastive	82.84	113 (0.66)	67.74	87.01	130 (0.61)	95.00	55.27	59 (0.82)	40.00	93.12	127 (0.62)	100.00	72.13	133 (0.60)	85.71
Qwen2.5-0.5B	Merged	82.54	114 (0.66)	67.74	87.53	138 (0.59)	95.00	69.90	89 (0.74)	69.90	94.86	149 (0.56)	100.00	72.13	133 (0.60)	85.71
Qwen2.5-7B	Path Patching	73.25	221 (0.72)	-	79.33	34 (0.95)	-	68.69	125 (0.84)	-	67.90	10 (0.99)	-	64.79	150 (0.81)	-
Qwen2.5-7B	Clean	9.38	195 (0.75)	41.17	30.29	195 (0.75)	52.94	2.02	195 (0.75)	41.60	77.46	148 (0.81)	50.00	36.45	195 (0.75)	47.33
Qwen2.5-7B	Contrastive	71.23	219 (0.72)	55.20	84.37	132 (0.83)	47.06	21.27	250 (0.68)	56.00	61.61	101 (0.87)	50.00	70.58	258 (0.67)	70.66
Qwen2.5-7B	Merged	82.09	303 (0.61)	74.38	88.03	232 (0.70)	67.65	70.92	317 (0.59)	61.60	93.03	206 (0.74)	60.00	73.57	336 (0.57)	79.33

Table 5: Comparing the performance, size and true positive ratio of Path Patching to pruning with vanilla FLAP, Contrastive FLAP and the resulting circuit of merging vanilla and Contrastive FLAP.

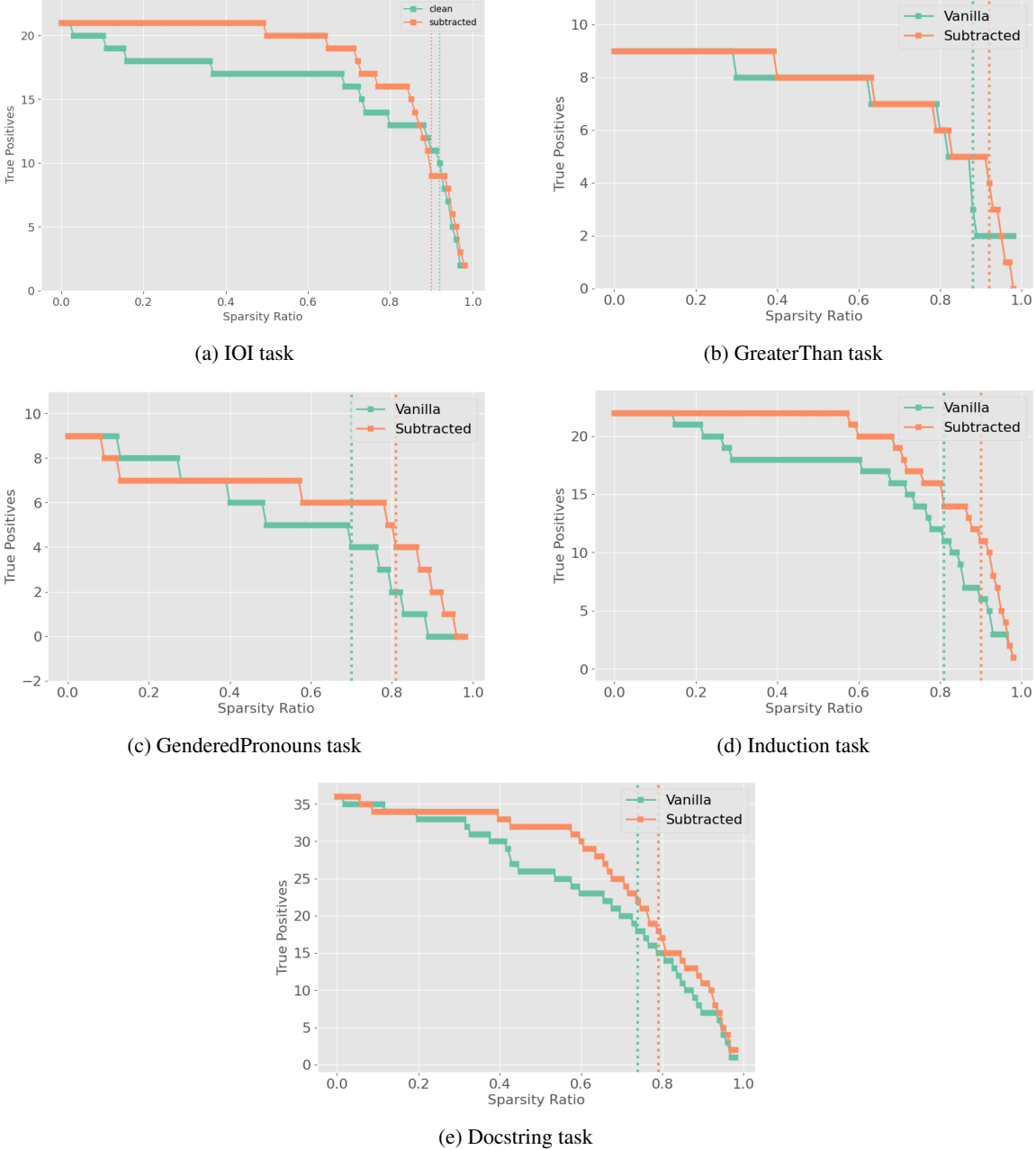


Figure 6: Amount of ground truth heads included by vanilla FLAP (green) and contrastive FLAP (orange). The dotted line shows the sparsity level at which the true positive reaches its **half-life value**.

	IOI	GreaterThan	GenderedPronouns	Induction	Docstring
Vanilla FLAP	0.92	0.88	0.70	0.81	0.74
Contrastive FLAP	0.90	0.92	0.81	0.87	0.79

Figure 7: Half-life values for Vanilla and Contrastive FLAP across all tasks

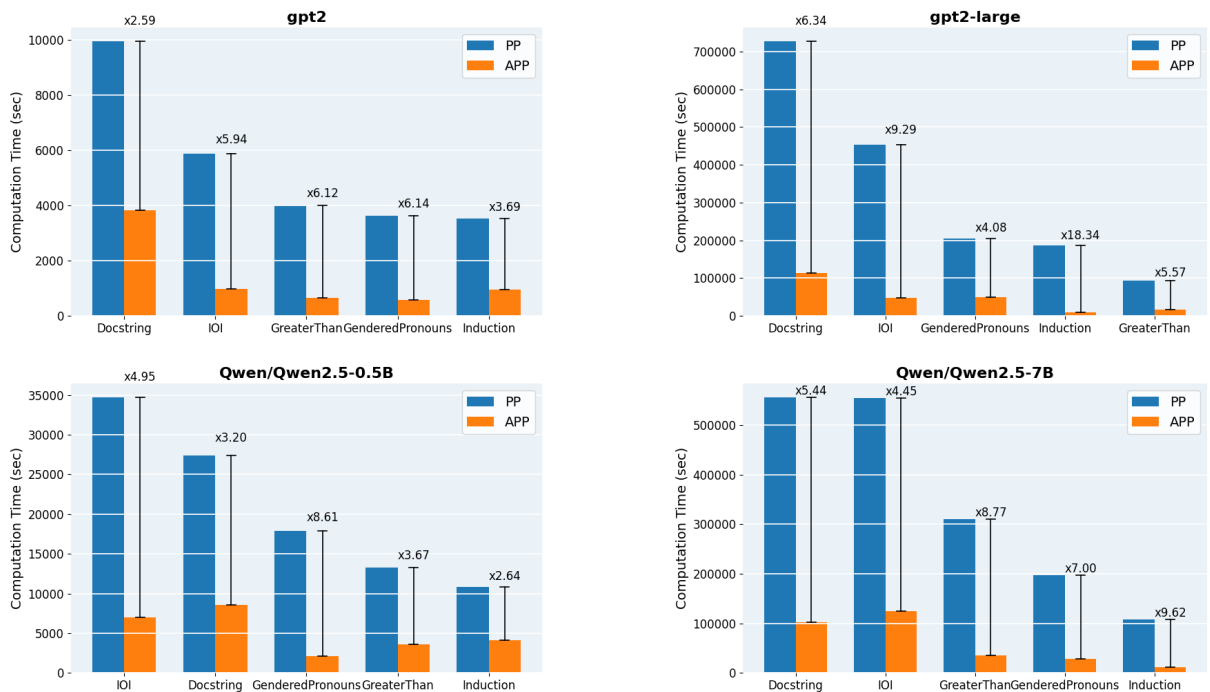
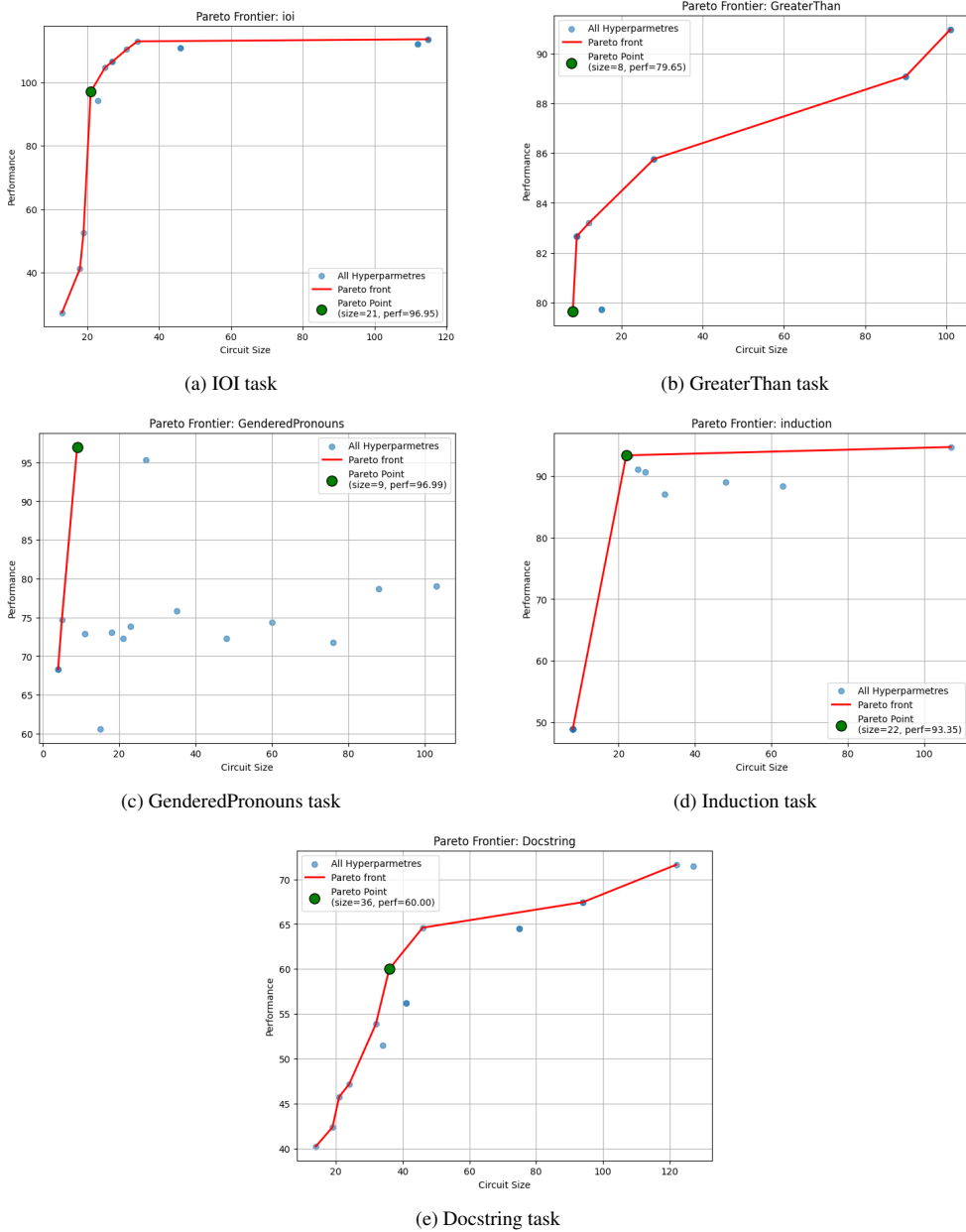


Figure 8: Difference of required computation time across all models and tasks

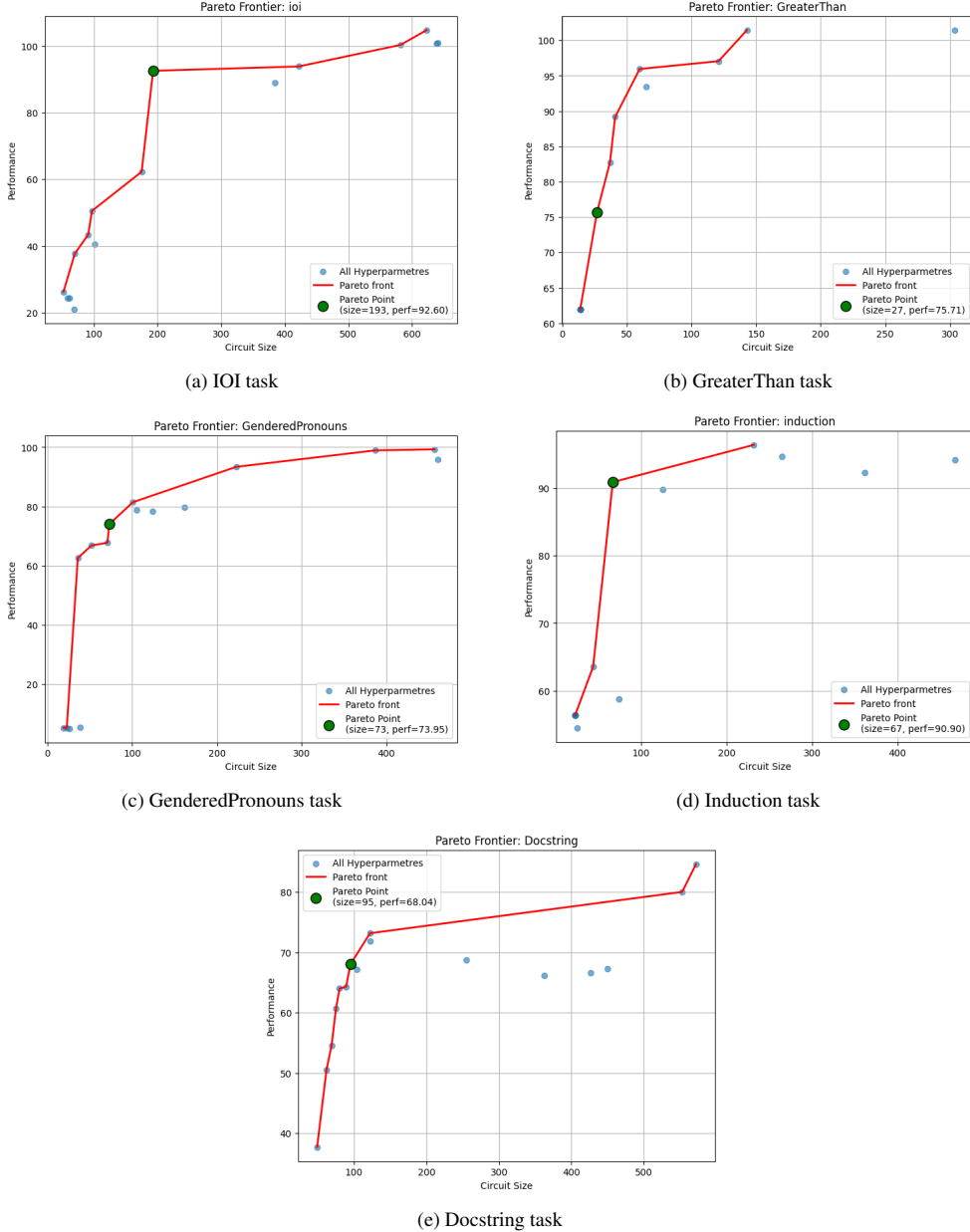
Automatic Path Patching: Hyperparameter testing for GPT-2 small



	Maximum Value	Importance	IOI P size	GreaterThan P size	GenderedPronouns P size	Induction P size	Docstring P size					
0.01	1		112.86%	34	83.20%	12	95.35%	27	48.95%	8	64.61%	46
	1.5		110.32%	31	82.67%	9	73.11%	18	48.95%	8	60.00%	36
	2		104.61%	25	82.67%	9	60.63%	15	48.95%	8	53.88%	32
	2.5		96.95%	21	79.65%	8	72.89%	11	48.95%	8	45.76%	21
0.001	1		113.51%	115	90.98%	101	79.04%	103	94.70%	107	71.45%	127
	1.5		112.01%	112	89.09%	90	71.77%	76	88.39%	63	67.45%	94
	2		110.84%	46	85.77%	28	72.29%	48	90.60%	27	64.48%	75
	2.5		106.4% 3	27	79.73%	15	73.88%	23	93.25%	23	56.21%	41
0.02	1		94.16%	23	82.67%	9	96.99%	9	48.95%	8	51.45%	34
	1.5		52.50%	19	82.67%	9	74.74%	5	48.95%	8	47.15%	24
	2		41.23%	18	79.65%	8	68.33%	4	48.95%	8	42.36%	19
	2.5		27.37%	13	79.65%	8	68.33%	4	48.95%	8	40.21%	14
0.002	1		113.51%	115	90.98%	101	78.70%	88	88.99%	48	71.64%	122
	1.5		112.01%	112	89.09%	90	74.35%	60	87.09%	32	67.45%	94
	2		110.84%	46	85.77%	28	75.86%	35	91.10%	25	64.48%	75
	2.5		106.43%	27	79.73%	15	72.29%	21	93.35%	22	56.21%	41

Figure 9: PP on GPT-2 small: Pareto points for each task are marked in bold.

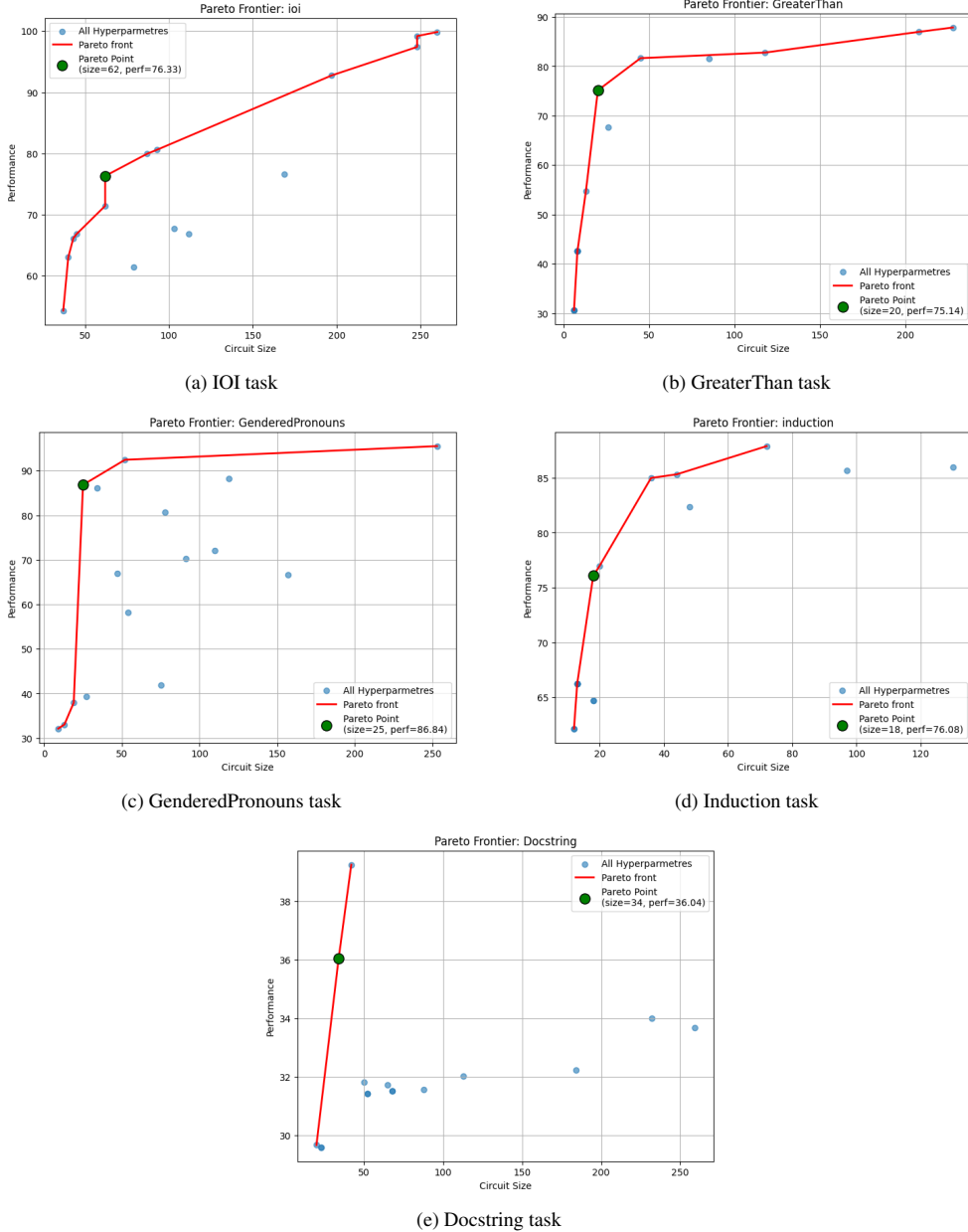
Automatic Path Patching: Hyperparameter testing for GPT-2 large



	Maximum Value	Importance	IOI P	size	GreaterThan P	size	GenderedPronouns P	size	Induction P	size	Docstring P	size
0.01	1		62.28%	175	61.97%	14	81.41%	101	56.39%	23	73.19%	122
	1.5		43.40%	91	61.97%	14	67.74%	71	56.39%	23	68.04%	95
	2		21.01%	69	61.97%	14	66.79%	52	56.39%	23	64.04%	80
	2.5		24.43%	62	61.97%	14	62.55%	36	56.39%	23	60.69%	75
0.001	1		101.06%	641	101.45%	304	95.79%	461	94.18%	467	67.32%	450
	1.5		104.84%	623	101.47%	143	79.58%	162	92.34%	362	66.61%	427
	2		100.39%	582	95.96%	60	78.29%	124	94.68%	265	68.75%	255
	2.5		93.91%	422	89.17%	41	73.95%	73	58.78%	74	67.21%	104
0.02	1		50.53%	97	61.97%	14	5.33%	39	56.39%	23	64.31%	89
	1.5		37.72%	70	61.97%	14	5.01%	26	56.39%	23	54.61%	69
	2		24.36%	58	61.97%	14	5.28%	23	56.39%	23	50.58%	62
	2.5		26.16%	52	61.97%	14	5.24%	19	54.50%	25	37.72%	49
0.002	1		100.87%	638	97.06%	121	99.25%	457	96.42%	232	80.04%	553
	1.5		92.60%	193	93.45%	65	98.91%	387	89.81%	125	66.23%	363
	2		89.02%	385	82.74%	37	93.35%	223	90.90%	67	71.93%	122
	2.5		40.59%	101	75.71%	27	78.70%	105	63.55%	44	84.65%	572

Figure 10: PP om GPT-2 large: Pareto points for each task are marked in bold.

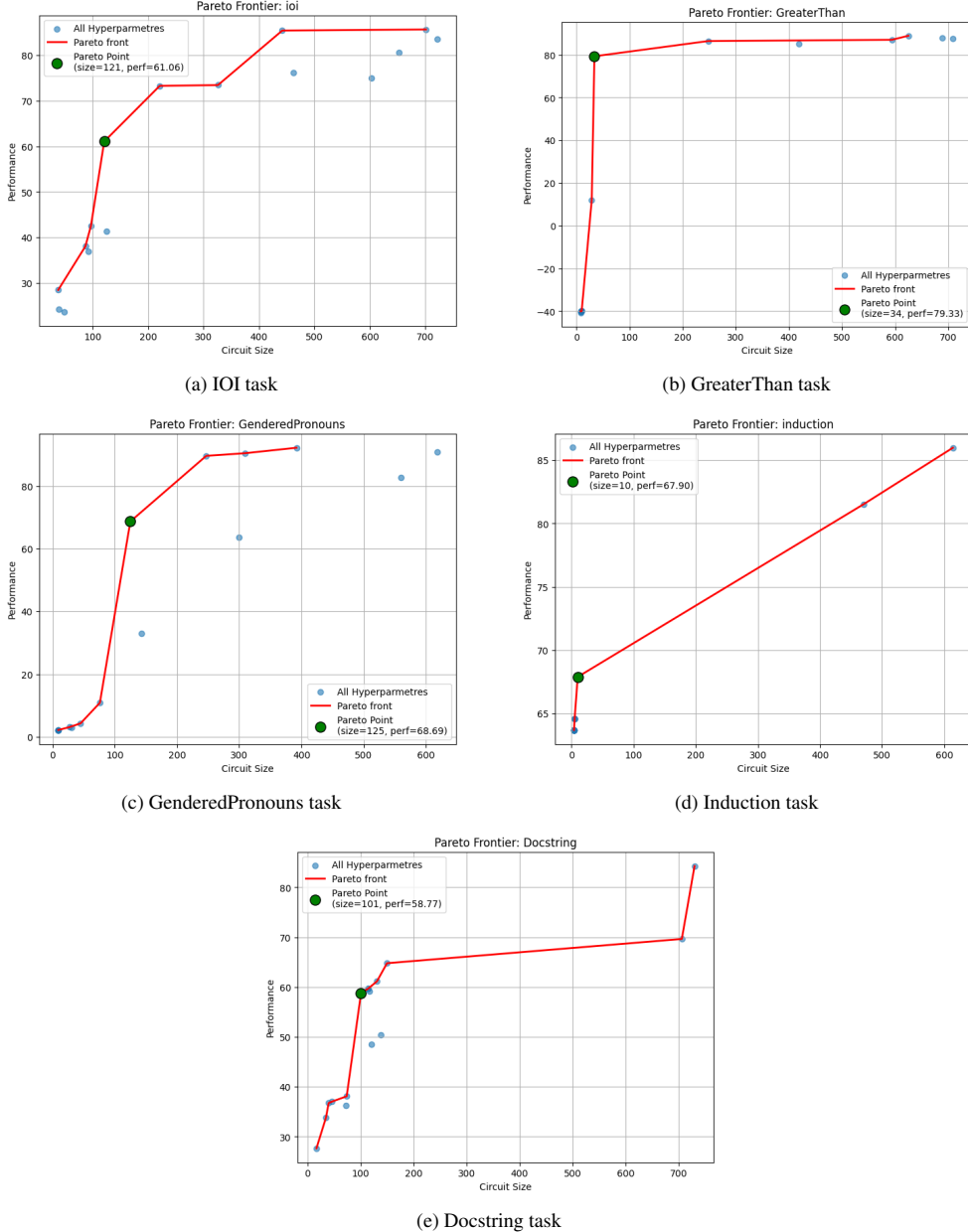
Automatic Path Patching: Hyperparameter testing for Qwen2.5-0.5B



		IOI	GreaterThan	GenderedPronouns	Induction	Docstring
	Maximum Value	Importance	P size	P size	P size	P size
0.01	1	80.62%	93	42.55%	8	70.29%
	1.5	76.33%	62	42.55%	8	92.46%
	2	66.86%	45	42.55%	8	86.20%
	2.5	63.05%	40	42.55%	8	86.84%
0.001	1	99.85%	260	87.86%	228	95.53%
	1.5	97.41%	248	86.98%	208	88.18%
	2	76.63%	169	81.60%	85	80.64%
	2.5	66.86%	112	67.66%	26	66.96%
0.02	1	79.96%	87	42.55%	8	39.27%
	1.5	76.33%	62	42.55%	8	37.92%
	2	66.16%	43	42.55%	8	33.04%
	2.5	54.33%	37	42.55%	8	32.11%
0.002	1	99.19%	248	82.79%	118	66.71%
	1.5	92.75%	197	81.66%	45	72.08%
	2	67.79%	103	75.14%	20	41.85%
	2.5	61.43%	79	54.76%	13	58.21%

Figure 11: PP on Qwen2.5-0.5B Pareto points for each task are marked in bold.

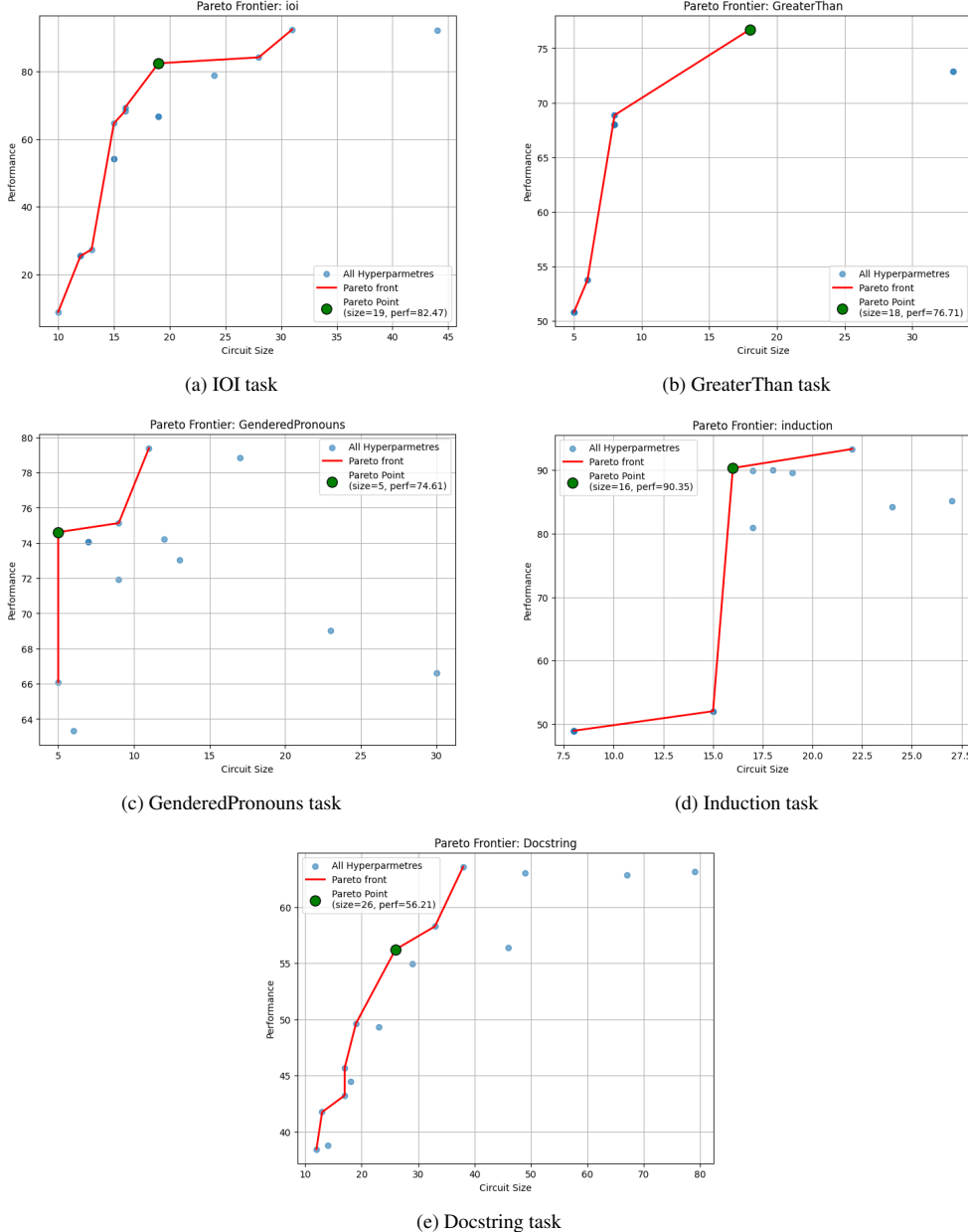
Automatic Path Patching: Hyperparameter testing for Qwen2.5-7B



	Maximum Value	Importance	IOI P	size	GreaterThan P	size	GenderedPronouns P	size	Induction P	size	Docstring P	size
0.01	1		73.25%	221	-39.98%	10	10.89%	76	63.71%	4	59.11%	117
	1.5		41.39%	125	-39.98%	10	4.34%	45	63.71%	4	58.77%	101
	2		42.55%	97	-39.98%	10	2.95%	31	63.71%	4	38.11%	74
	2.5		38.07%	87	-39.98%	10	3.12%	27	63.71%	4	36.26%	72
0.001	1		83.48%	721	87.72%	709	92.19%	392	85.97%	614	84.27%	730
	1.5		85.62%	701	87.88%	689	90.45%	309	81.51%	470	64.79%	150
	2		80.53%	652	87.05%	594	89.61%	247	67.90%	10	61.15%	131
	2.5		74.99%	602	86.45%	248	68.69%	125	67.90%	10	59.66%	114
0.02	1		37.03%	92	-40.06%	8	2.21%	9	63.71%	4	37.03%	46
	1.5		23.74%	49	-40.06%	8	2.21%	9	63.71%	4	36.75%	40
	2		24.23%	39	-40.06%	8	2.21%	9	63.71%	4	27.68%	17
	2.5		28.51%	38	-40.69%	9	2.21%	9	64.57%	5	33.86%	35
0.002	1		76.08%	462	88.93%	625	90.75%	618	64.57%	5	69.65%	706
	1.5		73.43%	326	85.18%	419	82.64%	560	63.71%	4	50.44%	138
	2		85.38%	442	79.33%	34	63.61%	300	63.71%	4	48.57%	121
	2.5		61.06%	121	12.08%	29	33.00%	143	64.57%	5	59.66%	114

Figure 12: PP on Qwen2.5-7B: Pareto points for each task are marked in bold.

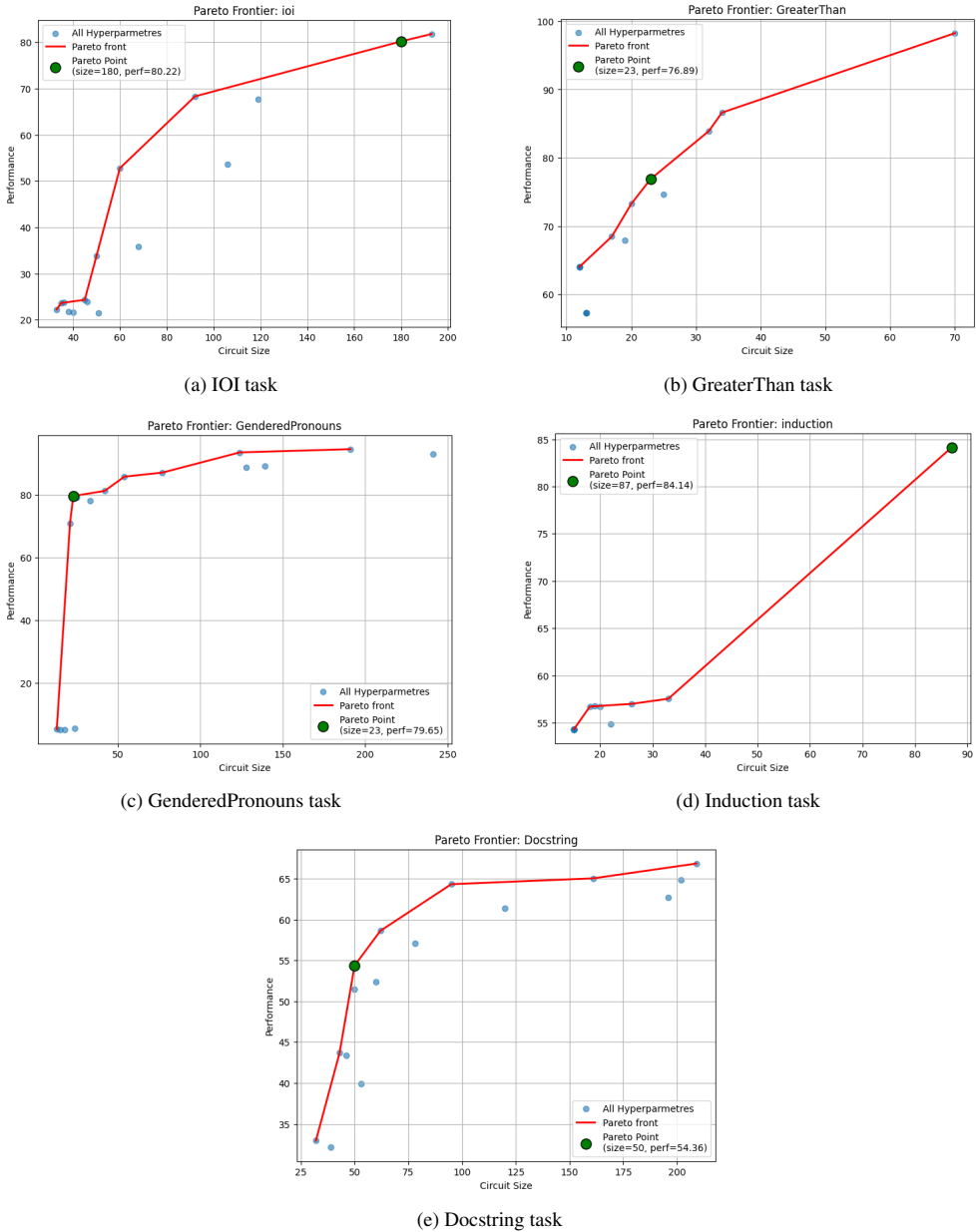
Accelerated Path Patching: Hyperparameter testing for GPT-2 small



Maximum Value	Importance	IOI		GreaterThan		GenderedPronouns		Induction		Docstring	
		P	size	P	size	P	size	P	size	P	size
0.01	1	82.47%	19	68.86%	8	79.39%	11	52.03%	15	56.21%	26
	1.5	68.31%	16	68.86%	8	71.94%	9	52.03%	15	49.64%	19
	2	69.35%	16	50.81%	5	63.34%	6	48.95%	8	38.79%	14
	2.5	64.68%	15	50.81%	5	66.09%	5	48.95%	8	38.45%	12
0.001	1	92.14%	44	72.86%	33	66.61%	30	84.24%	24	63.03%	49
	1.5	92.47%	31	76.71%	18	69.02%	23	89.89%	17	58.27%	33
	2	66.82%	19	68.03%	8	74.23%	12	90.35%	16	49.33%	23
	2.5	54.25%	15	68.03%	8	74.05%	7	89.64%	19	43.24%	17
0.02	1	27.37%	13	53.76%	6	74.61%	5	48.95%	8	54.94%	29
	1.5	25.45%	12	53.76%	6	74.61%	5	48.95%	8	44.48%	18
	2	25.45%	12	50.81%	5	74.61%	5	48.95%	8	41.76%	13
	2.5	8.87%	10	50.81%	5	74.61%	5	48.95%	8	45.70%	17
0.002	1	84.22%	28	72.86%	33	78.83%	17	85.19%	27	63.15%	79
	1.5	78.83%	24	76.71%	18	73.02%	13	93.35%	22	62.85%	67
	2	66.82%	19	68.03%	8	75.13%	9	90.05%	18	56.36%	46
	2.5	54.25%	15	68.03%	8	74.05%	7	80.94%	17	63.58%	38

Figure 13: APP on GPT-2 small: Pareto points for each task are marked in bold. In red are the circuits discovered by PP.

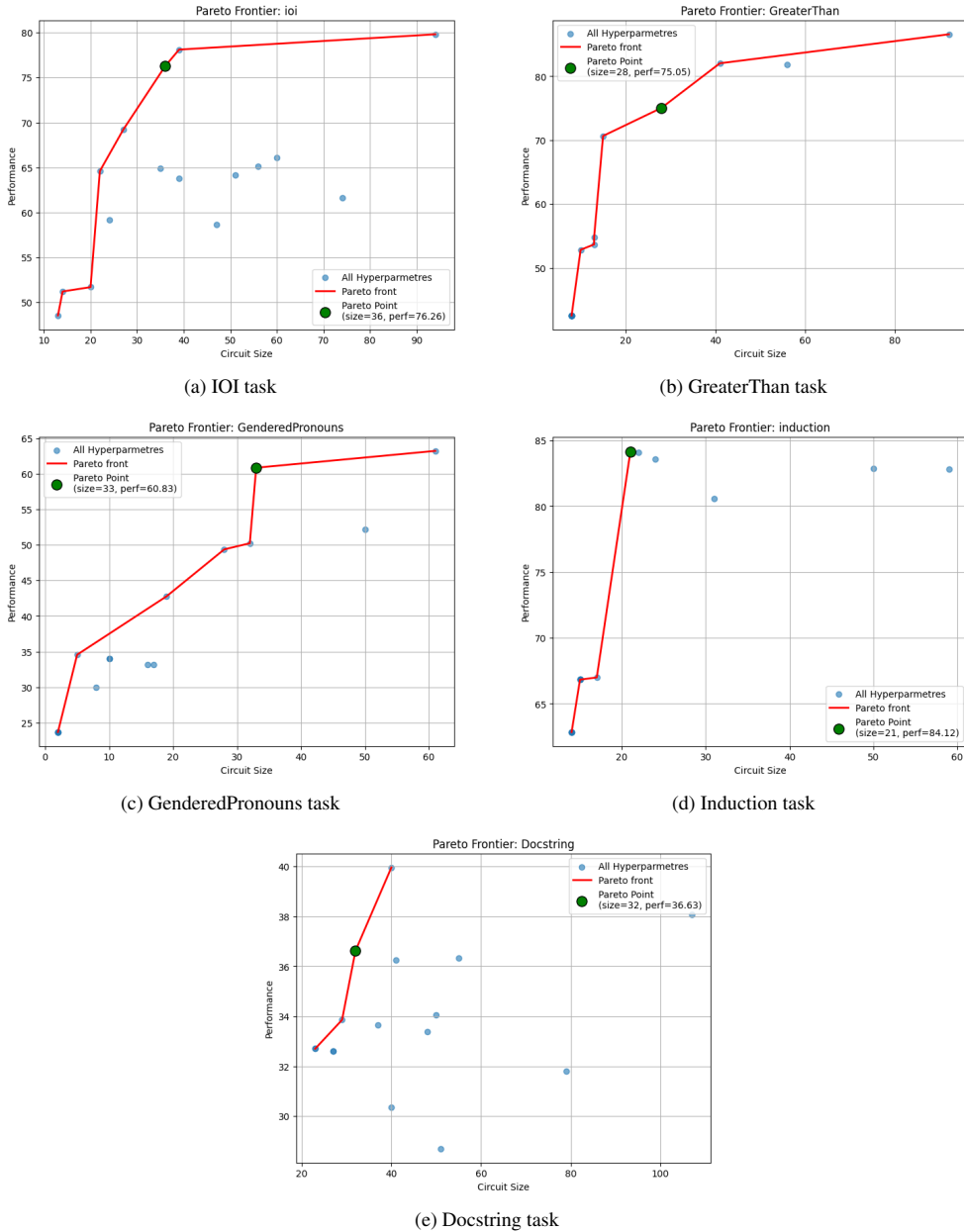
Accelerated Path Patching: Hyperparameter testing for GPT-2 large



Maximum Value	Importance	IOI P	IOI size	GreaterThan P	GreaterThan size	GenderedPronouns P	GenderedPronouns size	Induction P	Induction size	Docstring P	Docstring size
0.01	1	21.53	51	57.33	13	78.22	33	54.30	15	58.61	62
	1.5	24.34	45	57.33	13	79.10	25	54.30	15	54.36	50
	2	21.81	38	64.04	12	79.65	23	54.30	15	43.37	46
	2.5	23.68	35	64.04	12	70.90	21	54.30	15	43.67	43
0.001	1	81.82	193	98.25	70	92.94	241	84.14	87	66.83	209
	1.5	80.22	180	86.61	34	94.57	191	57.53	33	64.80	202
	2	67.70	119	76.89	23	93.55	124	56.98	26	62.72	196
	2.5	52.80	60	67.94	19	88.67	128	54.85	2	51.48	50
0.02	1	23.94	46	57.33	13	5.52	24	54.30	15	52.41	60
	1.5	21.66	40	57.33	13	5.28	18	54.30	15	39.94	53
	2	22.26	33	64.04	12	5.25	15	54.30	15	32.18	39
	2.5	23.72	36	64.04	12	5.32	13	54.30	15	32.95	32
0.002	1	68.33	92	83.93	32	89.28	139	56.69	20	65.02	161
	1.5	53.68	106	74.68	25	87.11	77	56.73	19	64.31	95
	2	35.83	68	73.26	20	85.82	54	56.68	18	57.07	78
	2.5	33.80	50	68.48	17	81.28	42	54.30	15	61.35	120

Figure 14: APP on GPT-2 large: Pareto points for each task are marked in bold.

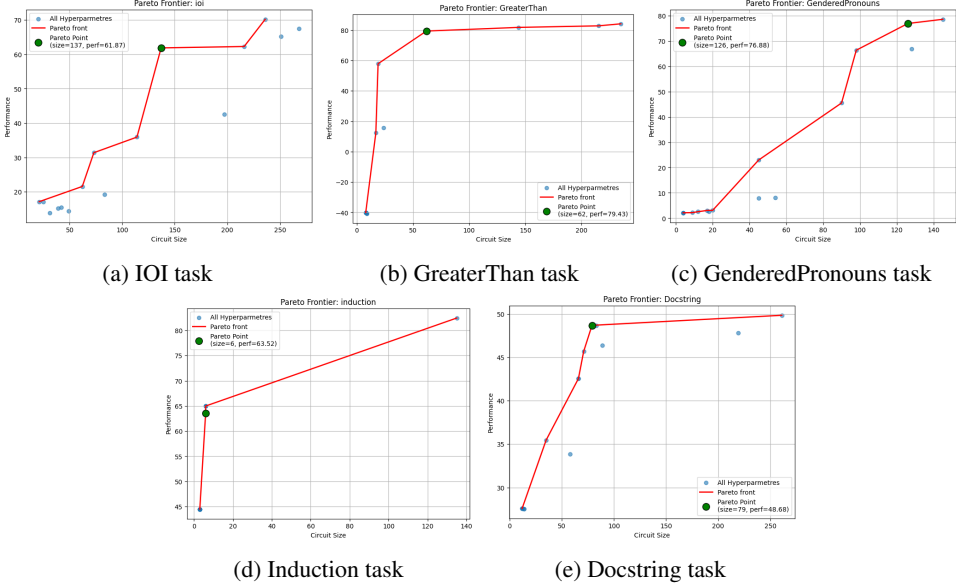
Accelerated Path Patching: Hyperparameter testing for Qwen2.5-0.5B



	Maximum Value	Importance	IOI P size	GreaterThan P size	GenderedPronouns P size	Induction P size	Docstring P size
0.01	1	78.11	39	42.55	8	49.36	28
	1.5	69.19	27	42.55	8	42.78	19
	2	64.61	22	42.55	8	29.98	8
	2.5	51.22	14	42.55	8	34.57	5
0.001	1	61.61	74	86.57	92	63.19	61
	1.5	58.65	47	81.79	56	60.83	33
	2	62.13	43	75.05	28	33.16	17
	2.5	63.79	39	53.67	13	34.06	10
0.02	1	76.26	36	42.55	8	23.71	2
	1.5	59.17	24	42.55	8	23.71	2
	2	51.70	20	42.55	8	23.71	2
	2.5	48.56	13	42.55	8	23.71	2
0.002	1	79.81	94	82.03	41	52.17	50
	1.5	66.09	60	70.66	15	50.22	32
	2	64.13	51	54.76	13	33.19	16
	2.5	64.94	35	52.83	10	34.06	10

Figure 15: APP on Qwen2.5-0.5B: Pareto points for each task are marked in bold.

Accelerated Path Patching: Hyperparameter testing for Qwen2.5-7B



Maximum Value	Importance	IOI P size	GreaterThan P size	GenderedPronouns P size	Induction P size	Docstring P size
0.01	1	19.27	83	-40.06	8	4.20
	1.5	21.58	62	-40.06	8	3.01
	2	14.49	49	-40.06	8	3.08
	2.5	15.44	42	-40.06	8	3.04
0.001	1	67.48	268	84.20	235	78.54
	1.5	65.16	251	82.86	215	66.83
	2	62.28	216	81.84	144	45.49
	2.5	35.93	114	57.92	19	8.00
0.02	1	15.18	39	-40.06	8	2.19
	1.5	17.16	25	-40.06	8	2.19
	2	17.16	21	-40.06	8	2.19
	2.5	13.92	17	-40.09	8	2.19
0.0001	1	42.61	197	79.43	62	76.88
	1.5	70.19	236	15.84	24	66.34
	2	61.87	137	12.42	17	22.97
	2.5	31.40	73	-40.69	9	7.94

Figure 16: APP on Qwen2.5-7B: Pareto points for each task are marked in **bold**. The highlighted row corresponds to the Path Patching configuration.